Characterization of metal ion-nucleic acid interactions in solution

Pechlaner, Maria ; Sigel, Roland K O

Abstract: Metal ions are inextricably involved with nucleic acids due to their polyanionic nature. In order to understand the structure and function of RNAs and DNAs, one needs to have detailed pictures on the structural, thermodynamic, and kinetic properties of metal ion interactions with these biomacromolecules. In this review we first compile the physicochemical properties of metal ions found and used in combination with nucleic acids in solution. The main part then describes the various methods developed over the past decades to investigate metal ion binding by nucleic acids in solution. This includes for example hydrolytic and radical cleavage experiments, mutational approaches, as well as kinetic isotope effects. In addition, spectroscopic techniques like EPR, lanthanide(III) luminescence, IR and Raman as well as various NMR methods are summarized. Aside from gaining knowledge about the thermodynamic properties on the metal ion-nucleic acid interactions, especially NMR can be used to extract information on the kinetics of ligand exchange rates of the metal ions applied. The final section deals with the influence of anions, buffers, and the solvent permittivity on the binding equilibria between metal ions and nucleic acids. Little is known on some of these aspects, but it is clear that these three factors have a large influence on the interaction between metal ions and nucleic acids.

DOI: https://doi.org/10.1007/978-94-007-2172-2_1

1

Characterization of Metal Ion-Nucleic Acid Interactions in Solution

Maria Pechlaner and Roland K. O. Sigel

Institute of Inorganic Chemistry, University of Zürich,
Winterthurerstrasse 190, CH-8057 Zürich, Switzerland
<roland.sigel@aci.uzh.ch>

ABSTRACT: Metal ions are inextricably involved with nucleic acids due to their polyanionic nature. In order to understand the structure and function of RNAs and DNAs, one needs to have detailed pictures on the structural, thermodynamic, and kinetic properties of metal ion interactions with these biomacromolecules. In this review we first compile the physicochemical properties of metal ions found and used in combination with nucleic acids in solution. The main part then describes the various methods

developed over the past decades to investigate metal ion binding by nucleic acids in solution. This includes for example hydrolytic and radical cleavage experiments, mutational approaches, as well as kinetic isotope effects. In addition, spectroscopic techniques like EPR, lanthanide(III) luminescence, IR and Raman as well as various NMR methods are summarized. Aside from gaining knowledge about the thermodynamic properties on the metal ion-nucleic acid interactions, especially NMR can be used to extract information on the kinetics of ligand exchange rates of the metal ions applied. The final section deals with the influence of anions, buffers, and the solvent permittivity on the binding equilibria between metal ions and nucleic acids. Little is known on some of these aspects, but it is clear that these three factors have a large influence on the interaction between metal ions and nucleic acids.

KEYWORDS: metal ions · ribozymes · RNA · methods · equilibrium constants

1. INTRODUCTION

Due to their polyanionic nature nucleic acids are unthinkable to exist without the close association of cationic counterions. Already the formation of secondary structures depends on the presence of metal ions because it requires the negatively charged backbones to come close to each other [1,2]. Larger RNAs form complicated tertiary structures with patches and cavities of increased negative electrostatic potential [3,4] that can not be stable without charge neutralization by associated cations. Most of the time, these ions are merely part of a diffuse ion atmosphere, providing the necessary charge neutralization but not interacting directly with the nucleic acid. Such ions can be well described by electrostatic continuum models based on the non-linear Poisson-Boltzmann (NLPB) equation [5]. A very small fraction of metal ions is coordinated tightly in buried binding pockets, where they are forced to release part or all of their hydration shells. In between the two extremes are those metal ions that interact with specific nucleic acid environments via a network of hydrogen bonds formed with their inner-shell water ligands and those, that are localized momentarily at electrostatically favorable sites like the major groove of RNA [3]. The wealth of loosely associated metal ions makes it difficult to single out the few more specifically bound metal ions.

It does not help that affinities even for the more selective and specific metal ion binding sites in nucleic acids are usually low (10^2 and 10^4 M^{-1} [6–8]) compared to those observed in

proteins. Typically most of the coordination sites in an RNA will have very similar metal affinities and are therefore filled more or less simultaneously [7,9,10]. In addition, metal ions bound to nucleic acids usually keep at least a part of their hydration shell, which is rather an exception in proteins, and fast exchange with the solvent is a common feature. Thus, the very dynamic nature of nucleic acids is also reflected in the characteristics of their interactions with metal ions. Consequently, approaches that work very well for metal ion-protein binding are often not appropriate or not even possible for nucleic acids. Clearly, a much higher emphasis has to be set on the thermodynamics and kinetics as opposed to the structural features. The verification of conclusions derived from the solid state and crystal structures is of particular importance, if they are to be transferred to the solution state.

Having said the above, a few more words on the importance of metal ion-nucleic acid interactions are necessary. Metal ions have stabilizing roles in DNA and RNA, but can also be responsible for large conformational changes. They can induce bending and unwinding [11,12] of nucleic acids. In addition, they are triggers for the B- to Z-transition in DNA (see also Chapter 3) [13–16]. G-rich sequences in telomeres and in the untranslated regions (UTRs) close to genes form G-quadruplex structures with the help of metal ions (see Chapter 4), for which regulatory roles in replication, transcription, and translation are suspected [17]. Similarly, a Mg^{2+}-sensing riboswitch in the 5'UTR regulates gene expression connected to metal homeostasis [18,19]. Apart from their structural role, coordinated metal ions are also often closely linked to the catalytic function of ribozymes. While it is not easy and not always possible to separate their structural and catalytic roles, metal ions have been identified in the active sites of most studied ribozymes (see e.g., [20–23]) and DNAzymes (see Chapter 8). Furthermore, they may be directly or indirectly involved in catalysis. The limited diversity of functional groups present in the four nucleotide building blocks of nucleic acids can be extended through the influence of metal ions [24], which can lead to a redistribution of electron densities, the shifting of pK_a values [25–30], the favoring of transition state geometries or the stabilization of rare tautomers [29,31].

It becomes thus evident how important a comprehensive knowledge is about the architectural, thermodynamic, and kinetic properties of metal ion-nucleic acid interactions for the understanding of the structure and function of nucleic acids. After a short introduction of the key

players, the involved metal ions (Section 2) and the nucleic acid ligating groups (Section 3), various methods, that have been employed in the characterization of coordination sites, binding kinetics, and binding affinities will be summarized and discussed (Sections 4, 5, and 6).

2. LIGATING SITES FOR METAL IONS IN NUCLEIC ACIDS

Metal ion coordination is influenced to a good part by the relative softness/hardness of potential metal ions and ligands, a concept that holds qualitative information on the electronegativity and polarizability of the groups [32,33]. Hard metal ions find suitable binding sites in the negatively charged non-bridging phosphate oxygens of the backbone and also in the exocyclic nucleobase oxygens [34], while the endocyclic nitrogens of the nucleobases are a preferred target of softer metal ions (Figure 1) [8,34–38]. Also available are the bridging phosphate oxygens and the 2'-hydroxyl groups of sugar moieties [39,40]. The exocyclic amino groups of the nucleobases are usually not suitable liganding sites because of the delocalization of the lone pair into the aromatic ring.

Steric factors also play a role, since especially in double-stranded helical regions some functional groups become inaccessible. In addition, the high rotameric freedom of the sugar-phosphate backbone, which in principle permits the formation of bi- and tridentate macrochelates, is more restrained in double-stranded regions.

insert Figure 1 close to here (width: 11.5 cm)

3. METAL IONS TO BE CONSIDERED TO INTERACT WITH NUCLEIC ACIDS

In the cell, kinetically labile metal ion-nucleic acid complexes predominate, which is to a large part due to the nature of the metal ions that are most abundant and freely available in the cellular environment (Table 1) [41–44]. Kinetically stable complexes on the other hand are employed in contexts procured by humans, like the administration of drugs or the development of nano-devices.

insert Table 1 close to here

3.1. Natural Metal Cofactors

3.1.1. Dominance of Mg^{2+}

Mg^{2+} is the most important cofactor of nucleic acids inside the cell [24,37,45–49]. It is also the most abundant divalent metal ion inside the cell (Table 1), but this is not the only factor that predestines it for its role in nucleic acid structure and function. Mg^{2+} is a relatively hard Lewis base with a small ionic radius and correspondingly a high charge density. It has a strong preference for oxygen ligands, especially charged ones. In octahedral complexes the distances between the six oxygen ligands are close to their van-der-Waals radii, resulting in an exceptional stability [50]. This leads to reduced solvent exchange rates and increased solvation enthalpy, but at the same time also makes it a most suitable interaction partner for the non-bridging phosphoryl oxygens of the nucleic acid backbone, allowing them to pack particularly closely [51], which is a prerequisite for the physiological folding of large RNAs. In accordance, a nearly perfect correlation between the cleavage rate of the hammerhead ribozyme [52,53] and the metal ion affinity towards phosphate monoesters can be established [34]. Nevertheless, such a correlation cannot be established, for example, for the *glmS* ribozyme [54], indicating a crucial influence of further ligand sites.

Partial dehydration of Mg^{2+} is enthalpically costly and so direct coordination contacts to nucleic acids are only favorable when more than one ligand in a suitable geometry replaces the water molecules [55,56]. Therefore, it is far more common that Mg^{2+} interacts through outersphere contacts of its first hydration shell, especially in the case of the nucleobase sites like the endocyclic nitrogens and exocyclic oxygens [57].

3.1.2. Monovalent Ions

In terms of abundance, Mg^{2+} is surpassed by the monovalent K^+, which is present in the cell at 140 mM, but also by Na^+ present at 10 mM concentration, a value comparable to that of Mg^{2+}. Outside the cell Na^+ and K^+ concentrations are reversed (Table 1). These monovalent ions are far less apt to establish a close packing of the negative charges of the nucleic acid backbone. Usually a largely unspecific role as general charge screeners is attributed to K^+ and Na^+, even if there are also examples of specific monovalent ion binding sites (Figure 2) [58,59].

insert Figure 2 in color close to here (width: 11.5 cm)

3.1.3. Influences of Metal Ions Other than Mg^{2+} and K^+

Na^+ and Ca^{2+} levels in the cell are lower than those of Mg^{2+} and K^+. Na^+ is expected to share the task of unspecific charge screening together with K^+. Ca^{2+} is used as a signaling molecule in the cell and therefore it is tightly regulated, e.g., by the fast uptake into the endoplasmic reticulum (ER) and mitochondria [60]. Tightly controlled are also typical protein metal cofactors like $Fe^{2+/3+}$, Zn^{2+}, and $Cu^{+/2+}$ [41,61,62], with significant free cellular concentrations only in case of intoxication, disease or drug treatment [63]. Nonetheless, also low levels of a metal ion are able to influence nucleic acids if binding specificity and affinity are favorable, as is shown for example by the allosteric inhibition of a group II intron when 5% Ca^{2+} compete against 95% Mg^{2+} [64]. In the same way other low-abundance metal ions might be involved in the regulation of RNA function [34]. In the following, we will shortly mention some relevant metal ions that are frequently studied in association with nucleic acids, highlighting their distinctive properties with respect to Mg^{2+} or K^+. Those latter two unfortunately are hard to detect and to characterize by most methods due to their low molecular weight and spectroscopic silence and hence, a variety of metal ions has been used as substitutes in different settings.

The interactions of metal ions in general with nucleic acids are governed by complex stabilities according to the Irving-Williams series [65] and Martin's Stability Ruler [66,67], by the relative affinities for oxygen versus nitrogen ligands [8] and by first shell hydration enthalpies (Table 2) [10,68–78]. Ca^{2+}, for example, shares the preference of Mg^{2+} for phosphate oxygen ligands, but is larger in size and thus compatible with higher coordination numbers and a more loose packing of ligands. Ca^{2+} can inhibit Mg^{2+}-dependent enzymes and ribozymes (e.g., [64,79–82]). Li^+ has a charge density and ligand preference comparable to Mg^{2+}, but favors tetragonal geometries. Mn^{2+} on the other hand, which is very similar to Mg^{2+} regarding both size and preferred coordination geometry, has a more balanced affinity for nitrogen and oxygen ligands and a ligand exchange rate 100 times faster than Mg^{2+} (Table 2). It is used as a paramagnetic probe in EPR as well as NMR experiments. Cd^{2+} is a much softer metal ion and therefore much more likely to interact through innersphere contacts with nucleobase nitrogens. In addition, it also has a higher inclination to form macrochelates than the other metal ions

mentioned so far [37,57,83]. Cd^{2+} is significantly larger than Mg^{2+}, but its thiophilicity [84–86] makes it a popular choice for metal-rescue experiments with phosphorothioates despite a serious caveat [86]. Zn^{2+} is also very thiophilic and more similar in size to Mg^{2+}, but engages in variable coordination geometries [87]. Tl^{+} has been employed as a substitute for K^{+}, making use either of its thiophilicity or of the abundant spin 1/2 nucleus of $^{205}Tl^{+}$. The kinetically inert complex $[Co(NH_3)_6]^{3+}$ can be of help to probe $[Mg(H_2O)_6]^{2+}$ binding sites, even if binding affinity and hydrogen bonding capacities differ because of the higher charge and the nature of the ammonium ligands, respectively. $[Co(NH_3)_6]^{3+}$ is, e.g., found to bind to the major groove of tandem G·U wobble pairs (Figure 2d).

insert Table 2 close to here

(reduce font size such that it fits landscape-wise on the width of a page)

Metal ions other than Mg^{2+} have been shown to support catalysis of natural ribozymes, some even at increased reaction rates, like Mn^{2+}, Co^{2+}, Zn^{2+}, and Cd^{2+} in the case of the RzB and *Schistosoma Hammerhead* ribozymes [52,53] or Ca^{2+} in the case of the antigenomic form of the hepatitis delta virus (HDV) ribozyme [88]. While in the case of the two Hammerhead ribozymes, the observed cleavage rates correlate with the respective phosphate affinity of the metal ion applied [34], in the case of the *glmS* ribozyme, no such correlation is observed [54]. Although such "more exotic" metal ions do not occur freely in the cell and are usually employed under *in vitro* conditions above their physiological abundances, locally or in secluded compartments of the cell, metal ions like Zn^{2+} might also *in vivo* reach concentrations where the described effects become significant.

3.2. Expanding the Natural Metal Repertoire of Catalytic RNAs and DNAs

While on the one hand ribozyme catalysis is in many cases promoted by a variety of divalent metal ions or even monovalent ions alone, on the other hand so far only a limited subset of metal ions have been shown to be specifically required in naturally occurring ribozymes, a fact that seems surprising in light of the diverse metal ion binding capabilities and selectivities of various *in vitro* selected ribozymes and DNAzymes. The latter have been shown to discriminate against

Mg^{2+}, while selecting for Ca^{2+} [89–91], Cu^{2+} [92–94], Co^{2+} [95], Zn^{2+} [96], Mn^{2+} [94], Pb^{2+} [97], Ni^{2+} [98] or a small subgroup of transition metal ions [99]. By the same means extraordinarily selective DNA biosensors for various metal ions have been engineered [100,101] (see also Chapter 8).

3.3. Kinetically Stable Metal Ion Complexes

In Nature, the structural integrity and function of nucleic acids is maintained by metal ions with intermediate to fast water exchange rates (Table 2). Consequently, these ions also form kinetically rather labile complexes with RNA and DNA. The action of metal-based drugs, on the other hand, usually depends on the irreversible association of metal ion complexes to DNA. Following the historical discovery of the anticancer properties of *Cisplatin, cis*-$(NH_3)_2PtCl_2$ (Figure 2e) [102], many other Pt^{2+}, but also Pt^{4+}, Ru^{3+}, Ga^{3+} and Ti^{4+} complexes have been investigated (see also Chapters 2 and 7) with regard to their anticancer activity [103].

3.4. Metallated Nucleic Acids for Nanotechnology

DNA, as a self-assembling molecule, has long been of interest for nanotechnological applications. The addition of metal ions can switch nucleic acids between two conformations (e.g., from single- to double-strand, or from hairpin to duplex), which has been taken advantage of for designing biosensors for metal ions (e.g., [104–107] and Chapter 8) and recently even logical AND and OR gates [108]. Furthermore, metal ions can modify the physico-chemical properties of nucleic acids and thereby extend their natural functional repertoire. While DNA alone possesses only marginal conductivity, one idea is that the incorporation of metal ions to natural or artificial nucleotides in double-stranded nucleic acid structures might yield useful molecular wires or magnets [109].

Incorporation of metal ions such as Zn^{2+}, Co^{2+}, or Ni^{2+} into DNA yielding so-called M-DNA has been proposed to make DNA more conductive [110–112]. There is still some controversy about this [113] as well as about the definite structure of M-DNA and the situation of metals therein [114–116].

In contrast, the structure of Hg^{2+}- and Ag^{+}-mediated base pairs, where the metal replaces the imino protons at the N3 position in U-U/T-T base pairs or stabilizes C-C mismatches, respectively, has been well established by NMR measurements and UV melting studies [104,117–119]. The binding of an Au^{3+} ion in the center of a G-C base pair has been observed in the crystal structure of an RNA [120].

The incorporation of artificial nucleotides that can serve as metal ion binding sites can help to fine-tailor the conformation and stabilities of nucleic acid structures. For instance, Müller, Sigel, and coworkers have demonstrated the incorporation of Ag^{+} ions into imidazole and triazole base pairs (Figure 2f) [118,121]. Clearly, with artificial nucleotides one can also further extend the range of possible metal binding sites. Examples are Cu^{2+}-hydroxypyridone base pairs [122] and salen metal base pairs (Cu^{2+}, $Mn^{2+/3+}$, Fe^{3+}, Ni^{2+}, and VO^{2+}) [123,124]. In a few cases artificial metal ion binding nucleotides have also been incorporated in polynucleotides with modified backbones like PNA (peptide nucleic acid; see also Chapter 12) and GNA (glycol nucleic acid) (see [125] and references therein). For a more detailed discussion on artificial base pairs we refer the reader to Chapters 10 and 11 of this volume and recent reviews by Müller and Clever and Shionoya [125,126].

4. STRUCTURAL CHARACTERIZATION OF METAL ION BINDING SITES

As summarized in the above section, the range of metal ions that have been observed to interact with nucleic acids in one or another specific context is very wide. The structural characterization of their binding sites, their precise localization, and the number and type of associated ligands in solution have been studied by a combination of chemical, biochemical and spectroscopic methods that will be discussed in the following.

4.1. Chemical and Biochemical Methods

Well-established biochemical and chemical methods are used to map metal ion binding sites through backbone cleavage. However, information on structural features of the interaction sites can be inferred only indirectly, by studying the effect on ribozyme kinetics or conformation of

mutated functional groups or the substitution of hard ligands or metals by soft ones. Nonetheless, many metal ion binding sites could be predicted by these methods, which only later on were confirmed in X-ray crystal structures. The strength of chemical and biochemical methods lies in the identification and characterization of catalytically important metal ion binding sites in ribozymes and their applicability also to very large molecules.

4.1.1. Metal Ion-Induced Hydrolytic Cleavage

Many metal ions catalyze the cleavage of phosphodiester bonds. The cleavage pattern in a large RNA thus holds information about the location of metal ion binding sites. The cleavage depends on local geometry and is mainly thought to take place through an "in-line" nucleophilic attack of the metal at a 2'-hydroxyl group that is followed by transesterification (Figure 3) [127,128]. A 2',3'-cyclic phosphate and a 5′ hydroxyl group result of this cleavage, analogous to the reaction catalyzed by the small phosphodiester-cleaving ribozymes. The cleavage rates have been shown to be pH dependent, thus indicating the involvement of the metal hydroxides [129]. Mg^{2+} has a very low cleavage capacity at neutral pH (the pK_a of $Mg(H_2O)_6^{2+}$ is 11.4; Table 2) and consequently, transition metal and lanthanide ions are normally used as probes. Pb^{2+} is much more efficient than Zn^{2+} and Mn^{2+} [130], but all three have been used to localize metal-RNA interaction sites [131–134]. Lanthanide(III) ions are especially suitable and employed frequently as probes because their charge makes them bind rather tightly and pK_a values close to neutral facilitate efficient cleavage [135–137].

insert Figure 3 close to here (width: 11.5 cm)

Cleavage assays require 5'- or 3'-^{32}P-end-labeling of the RNA. The cleavage products are separated by denaturing PAGE and the cleavage patterns subsequently used to determine the binding sites. Conclusions, however, are not straightforward because different factors determine the sites of cleavage. Firstly, favorable backbone geometries for cleavage are more common in single-stranded and loop regions than in double-stranded helices [128,138]. On the other hand, strong relevant binding sites in a more rigid environment with an unfavorable geometry for in-line attack might be missed. Secondly, while lanthanide and transition metal ions often seem to bind at the same sites as Mg^{2+} [136], they still are able to adopt diverse coordination geometries

or have divergent ligand preferences. Hence, one might miss the most specific binding sites while non-Mg^{2+} binding sites might be detected. Competition experiments with Mg^{2+} can help to identify physiologically relevant binding sites, but they are not able to distinguish effects of structural changes induced by a Mg^{2+} binding non-competitively at a different site from effective lanthanide displacement by Mg^{2+}. Cleavage experiments are thus prone to false negative as well as false positive results, but in combination with other experiments can give valuable information.

4.1.2. Metal Ion-Induced Radical Cleavage

Alternatively, metal ion binding sites can be probed with Fe^{2+} [139], taking advantage of the Fenton reaction [140,141]. In the presence of H_2O_2 Fe^{2+} is oxidized to Fe^{3+} generating short-lived hydroxyl radicals that will lead to backbone cleavage in the near proximity of the $Fe^{2+/3+}$ binding sites. Fe^{3+} is then reduced again to Fe^{2+} by sodium ascorbate. Fe^{2+} compares well to Mg^{2+} in terms of radius and coordination geometry (Table 2) [142] and can compete for Mg^{2+} binding sites [139]. However, it has to be kept in mind that their different Pearson hardness will in many cases lead to divergent binding preferences.

4.1.3. Mutational Approaches to Determine Metal Ligands

Once putative binding sites have been determined, various nucleotide analogs [143] can help to identify more details about a coordination site. Functional groups of a specific nucleobase, sugar or phosphate moiety are modified or removed and the effect can be monitored, e.g., by looking at the metal ion cleavage pattern. Alternatively, the metal ion binding sites that are important for catalysis or essential for structural integrity can be inferred from the catalytic competence or overall conformation of the mutated nucleic acid as determined in enzymatic or electrophoretic mobility shift assays, respectively.

Nucleotide analogue interference mapping (NAIM) [144] is an efficient way to systematically probe the importance of RNA functional groups [10]. In combination with metal ion switch experiments this method is also useful in establishing putative metal ion binding sites (see Figure 4 and Section 4.1.4.) [145–148]. T7 RNA polymerase is used to randomly introduce phosphorothioate nucleotides or nucleotide analogs (NTPαS) at levels of less than one

substitution per transcript. Afterwards those mutants, in which activity or another screenable characteristic has been abolished, are separated from the pool of transcripts. Iodine cleavage and subsequent analysis on the gel reveal the positions of the mutated nucleotides [144].

insert Figure 4 close to here (width: 11.5 cm)

The method can, for example, be used to identify metal-coordinating phosphate groups through metal rescue as described below, with the restriction that only R_P phosphorothioates can be studied as T7 polymerase selects against the other diastereomer [149]. Basu et al. have used a combination of X-ray crystallography and NAIM to identify a monovalent metal ion binding site in the *Tetrahymena* ribozyme P4-P6 domain [58]. They showed the rescue of a 6-thioguanosine mutation by Tl^+, a thiophilic K^+ substitute.

4.1.4. Metal Ion Switch Experiments

The divergent ligand preferences of different kinds of metal ions are the basis of metal ion switch experiments. Mg^{2+} and Mn^{2+} prefer the harder oxygen ligands, while Cd^{2+}, Zn^{2+} and Pb^{2+} display a pronounced preference for the softer aromatic-nitrogen and especially sulfur sites [84–86,150,151]. Mutations that exchange oxygen for sulfur or nitrogen groups can significantly suppress Mg^{2+} binding, but the adverse effects can often be rescued by Cd^{2+} or Mn^{2+}. The method is especially useful in identifying catalytically involved metal ions (see also recent reviews [152] and [10]) and is usually thought to be limited to the analysis of directly coordinated metal ions. However, Basu and Strobel report the rescue of outerspherely coordinated binding sites by Mn^{2+} [153]. Since Mg^{2+} preferentially binds to phosphoryl oxygens, the most common mutation in this kind of experiment is the exchange of phosphates for phosphorothioates, but also 2'-OH substitution by NH_2 has been used [154].

Evaluation of metal rescue experiments is complicated by several possible adverse effects. Firstly, there are the inherent physico-chemical differences (e.g., size, hydrogen bonding, coordination geometry, electronegativity) not only of the switched metal ions but also of the switched ligands. Sulfur, for example, is larger than oxygen and thus the introduction of a phosphorothioate by itself can already alter local structure and/or distort a metal ion binding site. Secondly, ribozymes usually present many other possible interaction sites for the rescuing metal,

at which binding can influence the structure and function significantly. To exclude them as well as possible, experiments are normally performed against a background of Mg^{2+}. Evaluation is usually based on relative rate constants that take into account the catalytic rates of all four combinations of the unmodified and modified ribozyme with Mg^{2+} and with the rescuing metal ion (equation 1) [152,155].

$$k^{\mathrm{rel}} = \left(\frac{k_{\mathrm{M}^{2+},\mathrm{S/N}}}{k_{\mathrm{Mg}^{2+},\mathrm{S/N}}} \right) \left(\frac{k_{\mathrm{M}^{2+},\mathrm{O}}}{k_{\mathrm{Mg}^{2+},\mathrm{O}}} \right)^{-1} \qquad (1)$$

$k_{M^{2+},S/N}$ and $k_{Mg^{2+},S/N}$ are the rate constants of the modified ribozyme in the presence of the substituting metal ion or Mg^{2+}, respectively, and $k_{M^{2+},O}$ and $k_{Mg^{2+},O}$ the corresponding rates in the wild-type ribozyme. Using an approach termed thermodynamic fingerprint analysis (TFA) that combines metal ion rescue with kinetic analysis, Herschlag, Picirilli, and coworkers were able to establish how many metal ions are involved in catalysis by the *Tetrahymena* group I intron ([154] and more detailed descriptions in [152,156]). By examining the influence of mutations at several sites in the RNA substrate and the cofactor GTP both in the absence and presence of Mn^{2+}, the authors were able to determine three sites with different Mn^{2+} binding affinities, thereby confirming the presence of three different metal ions. In the case of the *Hammerhead* ribozyme, a thio-rescue experiment gave valuable clues about the structure of the transition state active site: The analysis of enzyme kinetics in single and double mutants in a thio-rescue experiment strongly supports a bridging metal ion between a previously described metal ion binding site and the cleavage site [157].

4.1.5. Kinetic Isotope Effect

Compared to the modifications mentioned in the previous paragraphs, substitution of an atom with a heavier isotope of the same element is a very small, but nonetheless detectable intrusion in a system. The substitution can have an enhancing or decreasing effect on a reaction and thereby reveal information about the transition state structure [158,159]. Recently, this method has been applied to the transition state of RNase P [160,161]. The detected $H_2{}^{18}O$ heavy isotope effect agrees perfectly with the results obtained from the Mg^{2+}-catalyzed cleavage of the model

compound 5′-*p*-nitrophenylphosphate (T5PNP). This indicates that the cleavage mechanism in RNase P involves the same transition state as in T5PNP, where the $H_2{}^{18}O$ is directly coordinated to the metal ion [160]. In the future the better availability of specifically ^{18}O-enriched nucleotides might open the field for a wider application [162,163].

4.2. Spectroscopic Methods

4.2.1. Electron Paramagnetic Resonance

Electron paramagnetic resonance (EPR) spectroscopy can be very useful for the characterization of metal ion-nucleic acid interaction in several ways. However, most EPR methods require the sample to be frozen. In solution at room temperature, EPR can provide information on the populations of free and bound metal ions and thereby binding affinities as well as cooperativities but structural details are not accessible [164–166]. At low temperature in a frozen sample, hyperfine interactions between the unpaired electron spin of a paramagnetic metal ion and the spin of the nuclei are able to hint at the coordination environment of the metal ion. Two more advanced applications, ENDOR (electron-nuclear double resonance spectroscopy) and ESEEM (electron spin echo envelope modulation) can even reveal details about the number and type ($^{14}N/^{15}N$, $^{1}H/^{2}H$, ^{31}P) of the immediate coordinating partners within a radius of 6–7 Å. For a more detailed description of the techniques we refer the interested reader to recent expert reviews by DeRose and coworkers [167,168].

Since EPR is limited to paramagnetic metal ions, Mn^{2+} is a popular object of study due to its similarities with Mg^{2+} (Table 2). Both its electron and nuclear spin are 5/2, but degeneration leads to a spectrum with only 6 characteristic main lines. The exchange of metal ion-coordinated water molecules for RNA ligands is accompanied by subtle perturbations of the spectrum. As signals from differently bound metal ions will always overlay, an unambiguous analysis usually requires sample conditions with only one prominent metal ion binding site. A single tightly bound Mn^{2+} ion can, for example, be observed in a background of monovalent ions in the *Hammerhead* ribozyme: ESEEM spectroscopy allowed the precise localization of the metal ion at a site with specifically ^{15}N-labeled guanine, the determination of further liganding sites and also of the hydration level [169]. In a different approach, multiple Mn^{2+} binding sites in the

Diels-Alder ribozyme were gradually silenced by Cd^{2+}, allowing thus their individual characterization [166].

4.2.2. Lanthanide(III) Luminescence

The luminescence of lanthanide(III) metal ions is sensitive to the direct coordination environment and thus can yield information on the metal ion binding pocket. This method is mentioned here for the sake of completeness but we refer the reader to Chapter 6 of this volume for a detailed description.

4.2.3. X-ray Absorption Spectroscopy

The coordination environment of tightly bound transition metal ions can be characterized in detail in solution by X-ray absorption spectroscopy (XAS) methods like XANES and EXAFS. XANES (X-ray absorption near edge structure) is sensitive to the average oxidation state of the metal in the sample, while EXAFS (extended X-ray absorption fine structure) allows the deduction of the number and type of ligands as well as coordination geometry and metal-ligand atom distances. Detection is possible in dilute solution and metal ions that are classified as spectroscopically silent (like Na^+, K^+, Mg^{2+}, or Ca^{2+}, Cu^+, and Zn^{2+}) are accessible [170].

Nucleic acids are not optimally suited for XAS investigations, considering the predominantly weak interactions and the coexistence of many metal ion binding sites in most constructs. Nonetheless, higher-affinity binding sites, like the ones in the G-quadruplex channel [171] or in a short RNase P helix P4 model [172] can be characterized in remarkable detail, not to forget complexes of kinetically more inert metal ions [173,174].

4.2.4. Vibrational Spectroscopies

Metal ion binding is reflected in changes of the vibrational bands of nucleobase, sugar, and phosphate constituents, which can be measured by infrared (IR) and Raman spectroscopy. While IR depends upon oscillating dipole moments and is influenced by all types of non-symmetrically bonded atoms, Raman signals derive from the inelastic scattering of photons and occur when there are changes in polarizability. The latter are therefore especially sensitive to electron-rich or multiply bonded groups. In addition, water absorbs in the IR range but is not observed in Raman

spectra. Thus, the two methods can yield useful complementary information on a fast timescale and in all physical states [175,176]. Discrete vibrational bands for base, sugar and phosphate groups can be observed, albeit only as an average signal of all conformational states in the sample. Isotopic labeling is an approach to partly alleviate this problem [177,178].

FT-IR (Fourier-transform infrared) spectroscopy and Raman spectroscopy have been employed to semiquantitatively follow metal ion-induced conformational changes [13,179,180] and identify primary binding sites for a variety of metal ions in RNA and DNA [181–187]. By Raman spectroscopy the largest metal ion-dependent changes are observed in the phosphodiester signals. The symmetric stretching of non-bridging phosphate oxygens has recently been proposed to contain quantitative information about the degree of innersphere coordinated metal ions in RNA [188]. Christian et al. [188] find that while electrostatic and hydrogen interactions yield only an attenuation, innersphere coordination is accompanied by a shift of the Raman signal, an effect that could in addition also be roughly correlated to the electronegativity and the Pearson hardness of the respective metal ion. Raman spectroscopy in solution requires rather concentrated and highly pure samples, restricting this method to the analysis of smaller constructs. Raman crystallography or microscopy is an approach that can significantly increase signal intensity and reduce background signals. It allowed the identification of inner- and outersphere coordinated metal ions in the HDV ribozyme [189–191].

4.2.5. Nuclear Magnetic Resonance Methods

Nuclear magnetic resonance (NMR) spectroscopy has provided the three-dimensional structures of hundreds of RNA and DNA molecules. Its restriction in terms of molecular size – compared to X-ray crystallography – is outweighed by the singular capacity to reveal not only structure and conformation, but also local and global dynamics of macromolecules in solution in a quantitative manner. The big advantage compared to other spectroscopic methods in solution is the resolution of the individual nuclei at almost every single position in a polynucleotide chain, allowing the simultaneous site-specific characterization of multiple metal ion binding sites.

Most approaches are based on indirect observations of metal ion induced changes in the nucleic acid binding sites. The most abundant isotopes of hydrogen and phosphorus (^{1}H and ^{31}P) both have nuclear spins of 1/2 as it is the case with ^{15}N and ^{13}C. The latter are widely used in

isotopically enriched nucleotides instead of the natural isotopes ^{14}N and ^{12}C. But also the direct observation of NMR-active metal nuclei can help in the structural and thermodynamic characterization of metal binding sites [192,193]. Metal ion-nucleic acid interactions can have repercussions on chemical shifts, relaxation properties and scalar couplings of involved NMR active nuclei [194]. In addition, NOEs (nuclear Overhauser effects) to the protons of popular metal ion mimics, $[Co(NH_3)_6]^{3+}$ and NH_4^+, can denote coordination sites [195].

4.2.5.1. Chemical Shift Perturbations: Chemical shifts are the most straightforwardly measurable factor in a NMR experiment (Figure 5). Binding of metal ions can influence the chemical shift in two ways: Either through direct deshielding of a nucleus or through shielding/deshielding effects upon conformational changes of the neighborhood that result from a binding event. The latter effect is especially prevalent for ^1H shifts and reduces the accuracy with which a binding site can be localized, but on the other hand it is also a highly sensitive flag to define the binding pocket. In the case of smaller structures that do not undergo significant conformational changes upon metal ion interaction, ^1H shift perturbations can be used as good indicators of metal ion binding sites [6,196,197]. Imino proton shifts are mostly well resolved and can often be monitored satisfactorily in 1D spectra. However, the observable ones are usually part of a Watson-Crick hydrogen bonding pattern and then not in close proximity to the metal ion binding atom. In addition, the chemical shift of imino protons is very sensitive to temperature and accessibility of bulk water, which may falsify results.

insert Figure 5 close to here (width: 11.5 cm)

(must fit on one page together with the legend)

In this case, homo- or heteronuclear 2D NMR spectra can often yield more significant shift perturbations from the non-exchangeable protons. Mg^{2+}-induced ^1H chemical shift changes are usually not larger than 0.1–0.2 ppm [6,7,197] at limiting metal concentrations of ~10–20 equivalents and perturbations of ^{13}C chemical shifts are similarly small in general [197–200]. Chemical shifts induced by $[Co(NH_3)_6]^{3+}$ are slightly more pronounced due to the higher charge and associated 10 times stronger binding affinity [201]. Unfortunately, exchange rates of commonly employed metal ions are often in the intermediate regime on the NMR time scale [84]

leading to a general broadening of the lines already at lower concentrations that can impede the analysis of chemical shift changes.

With ^{31}P, nucleic acids contain a second highly sensitive and abundant spin 1/2 nucleus in addition to protons, whose only disadvantage is the low signal dispersion. Most ^{31}P resonances cluster in the small region between –3 to –1 ppm and only a few with non-standard backbone torsion angles can be resolved from the rest [202]. ^{31}P resonances can be unambiguously assigned by the site-specific incorporation of a non-bridging ^{17}O that efficiently broadens the signal of the adjacent ^{31}P [203], an approach which has been employed, e.g., by Hansen et al. [204] to pinpoint a binding site in a *Hammerhead* ribozyme. Alternatively, ^{31}P resonances from the crowded bulk region can be resolved by the incorporation of phosphorothioates, which have a ^{31}P resonance shifted by ~60 ppm [203,205], allowing to observe effects of metal ion binding to selected sites in the phosphate backbone [206]. Coordination of Cd^{2+} to a phosphorothioate, for example, will lead to an upfield shift of the ^{31}P resonance by a few ppm in both R_P and S_P diastereomers, as has been observed for both the A9/G10.1 and scissile phosphate locations in the hammerhead ribozyme [207,208] in agreement with the results of biochemical studies by Wang et al. [157]. However, such experiments have to be interpreted with care because the introduction of a sulfur atom might also create a new or specially shifted binding site.

Considering the unfavorable NMR characteristics of oxygen isotopes, ^{15}N is the only nucleus in nucleic acids that can serve as a probe for the detection of an innersphere coordination site. In addition, ^{15}N is straightforwardly observable by NMR spectroscopy. This explains why with ^{15}N, compared to ^{1}H, ^{13}C and ^{31}P, much higher chemical shift perturbations can be observed. Direct coordination to nucleobase nitrogens is confirmed in Hg^{2+}-mediated thymine base pairs in DNA by 30 ppm ^{15}N downfield shifts [117] as well as by Ag^{+} coordination to imidazole nucleotides [118]. Also the more labile coordination of Cd^{2+} and Zn^{2+} ions to N7 induces 20 ppm shifts in 1D ^{15}N experiments [209–211]. An initial broadening of the ^{15}N resonance is attributed to the exchange between free and bound states. At higher, saturating Cd^{2+} concentrations the peak grows sharper again. Resonances for the adjacent purine ^{13}C8 and ^{1}H8 are perturbed less but still significantly [172], which is not observed in outersphere coordination [212,213]. Since direct observation of the low sensitivity nucleus ^{15}N can be lengthy, the

recording of 2D [^{1}H,^{15}N]-HSQC can be advantageous, while at the same time enhancing the resolution. On the basis of ^{2}J-[^{1}H,^{15}N]-HSQC experiments Erat et al. have proposed that the combined information of ^{1}H and ^{15}N shifts and characteristic broadening can be used to identify inner- and outersphere binding events [214]. The empirically collected knowledge agrees well with theoretical calculations, confirming that ^{15}N chemical shifts are a valid means to determine the coordination mode [215,216].

4.2.5.2. Paramagnetic Effects: The large magnetic moment of an unpaired electron of a paramagnetic metal ion species efficiently relaxes nuclei in their immediate environment (Figure 5b) [172,217,218]. The effect is strictly distance-dependent (relative to r^{-6}) and leaves less room for ambiguity than chemical shift perturbations. Paramagnetic line broadening information can even be included as weak distance restraints in molecular dynamics calculations [197]. Mn^{2+} exchanges very fast between the free and bound form and can therefore effectively relax a whole molecule at substoichiometric concentrations. µM amounts are usually enough to detect site-specific line-broadening effects. Mn^{2+} is most widely used because of its likeness to Mg^{2+} (e.g., [219–221]), but also Co^{2+} and Ni^{2+} are suitable paramagnetic probes [98,222].

4.2.5.3. NOE Crosspeaks to $[Co(NH_3)_6]^{3+}$ and NH_4^+: $[Co(NH_3)_6]^{3+}$ is a mimic for $[Mg(H_2O)_6]^{2+}$ [223] and has been used in a wide range of studies [172,200,201,224–226]. Similarly, NH_4^+ can be used as a substitute for monovalent metal ions [195]. Both compounds possess protons that are amenable for direct observation of inter-molecular NOE crosspeaks (Figure 5d) to nucleic acid protons in a radius smaller than 6 Å. In the most common case tumbling of the cation in the binding site and exchange with the unbound state are fast on the chemical shift time scale and all $[Co(NH_3)_6]^{3+}$/NH_4^+ protons resonate at a single frequency. G-quadruplex structures are an exception, displaying a binding site with on-off rates slow enough to allow observation of separate resonances for free and bound ammonium [227,228]. The tight binding even significantly slows down the usually fast proton exchange of ammonium [195]. It is advantageous to employ ^{15}N-labeled NH_4^+ because it not only avoids the quadrupolar ^{14}N nucleus, but also allows for heteronuclear HSQC experiments that detect the exchange of ions between binding sites and the solvent [229]. Structural information, however, can be inferred in

both fast and slow exchanging cases. From the NOE cross-peaks of $[Co(NH_3)_6]^{3+}$ or NH_4^+ weak distance restraints can be extracted and integrated in molecular dynamics simulations to infer binding sites [45].

4.2.5.4. Direct Detection of NMR-Active Metal Isotopes: A good number of the metal ions that have been studied in association with nucleic acids have at least one NMR-active isotope. Unfortunately many of them, including the biologically most relevant $^{23}Na^+$, $^{39}K^+$, and $^{25}Mg^{2+}$, have half-integer spins > 1/2. Fast quadrupolar relaxation usually restricts their use in solution NMR experiments to the study of kinetic and thermodynamic features by line shape analysis (see also Sections 5 and 6) [230–234] and pushes them more into the field of solid state NMR, which is better suited to handle the large quadrupolar effects.

Spin 1/2 isotopes are available in ^{52}Fe, ^{107}Ag, ^{109}Ag, ^{111}Cd, ^{113}Cd, ^{195}Pt, ^{199}Hg, ^{203}Tl, ^{205}Tl, and ^{207}Pb. Many have wide chemical shift ranges and can give useful information about coordination geometry and ligand atom identity, as has been shown in proteins [235,236]. In nucleic acids, however, their use is most often restricted by the problem of weak binding and fast exchange. An exception is again the high-affinity binding of monovalent metal ions to G-quadruplex structures that even permitted the direct observation of separate peaks for the bound and unbound species of $^{23}Na^+$, $^{39}K^+$, and $^{85}Rb^+$, which was not thought possible so far [192,237].

$^{205}Tl^+$ is a very useful NMR substitute for K^+ and Na^+ due to its high natural abundance (70%) and high sensitivity [238]. Basu et al. observe two well separated $^{205}Tl^+$ peaks for the bound and unbound species in a G-quartet [239]. In a subsequent work Gill et al. even managed to measure small scalar ^1H-$^{205}Tl^+$ couplings of < 1 Hz between the ion and imino and aromatic protons, which allow the precise localization of metal ions in a G-quadruplex structure [193].

Such direct couplings could not be observed between $^{113}Cd^{2+}$ and ^{15}N upon coordination of the metal ion to an N7 in the tandem G·A base-pair motif of the hammerhead ribozyme [209,212], which is attributed to the fast exchange of Cd^{2+}. The coordination of Ag^+ ions between imidazole nucleotide analogs in a DNA duplex on the other hand is stable enough to observe a 87 Hz $^1J(^{15}N,^{107/109}Ag)$ coupling indirectly in the splitting of the nitrogen signal (Figure 5c) [118].

5. DETERMINATION OF BINDING KINETICS

Metal ions interact with nucleic acids on a very wide range of time scales. Fast exchange (ms to µs range) dominates the dynamic interactions of the majority of alkali and alkaline earth metal ions. On the other extreme, metal complexes effective in cancer treatment are characterized by particularly slow kinetics that can be in the order of hours or days [240]. Mg^{2+} is special with regard to its water-ligand exchange rate of ~$2 \cdot 10^5$ s^{-1} being four orders of magnitude slower than that of most of the main group metal ions, but also significantly slower than many transition metal ions [241].

5.1. Nuclear Magnetic Resonance

The appropriate approach for establishing binding kinetics is determined by the association-dissociation rate of the metal ion, which can be fast, intermediate or slow on the respective time scale accessible to the employed method. For example, what is considered fast on the NMR (~10^{-1}–10^{-9} s) or EPR (~10^{-4}–10^{-8} s) time scale will still be slow in IR (~10^{-13} s) or UV (~10^{-15} s) spectroscopy [42]. In the case of slow exchange, separate signals can be observed for each exchanging species, while fast exchange only displays one averaged signal (Figure 6). NMR has proven the most versatile tool to determine thermodynamic and kinetic parameters on different time scales. Most of the relevant exchange processes in nucleic acids happen in fast exchange (> 10^3 s^{-1}) relative to the NMR chemical shift time scale. In this regime, the NMR signal has a chemical shift that corresponds to the population-weighted average of the chemical shifts of the bound and unbound forms. A concentration-dependent movement of the signal can be used to deduce affinity constants (see Section 5.2). If the exchange is moderately fast (too fast would be $k_{-1} > 40\ |\delta_{bound}-\delta_{unbound}|$ [242]) a full line-shape analysis can give on- and off-rates of metal binding as well as equilibrium dissociation constants [242,243]. Relaxation rates and line-shapes of the quadrupolar nuclei ^{23}Na, ^{25}Mg, and ^{43}Ca are modulated by their interactions with larger molecules and have been used in a number of studies to characterize binding kinetics, cooperativity and co-solute dependence [230–232,234,244–246].

insert Figure 6 close to here (width: 6 cm)

Magnetic relaxation dispersion (MRD) experiments allow the probing of molecular motions over a wide range of time scales by recording autorelaxation rates of quadrupolar nuclei at various different field strengths [247,248]. In this way the residence times of small molecules like H_2O (through ^{2}H or ^{17}O) [249] or metal ions (especially well suited is $^{23}Na^{+}$) on the surface of a biomolecule can be determined under fast exchange conditions. By MRD experiments, Halle and colleagues confirmed the binding of $^{23}Na^{+}$ in the minor groove of DNA A-tracts by showing that binding is blocked by the minor groove binding drug netropsin [250,251]. Results support the existence of relatively long-lived $^{23}Na^{+}$ (50 ns [250]; 10 ns to 100 µs [251]) and $^{58}Rb^{+}$ (0.2 ± 0.1 µs [251]) ions.

When NH_4^+ or $[Co(NH_3)_6]^{3+}$ are used as metal ion mimics, cross-relaxation experiments on the basis of the nuclear Overhauser effect (NOESY, ROESY) can be used to observe fast exchange between different binding sites and the solvent [11]. Together, the peak magnitudes and the absence of an observable change in the dominant bulk chemical shift of ammonium protons allow the deduction of upper and lower limits for the exchange rate, but no exact quantification.

Intermediate exchange is characterized by severely broadened resonances. As long as the resonances are still detectable, temperature-dependent changes and line-shape analysis can yield exchange rates. Mg^{2+} interactions with RNA often occur on an intermediate time scale leading to a gradual broadening of all resonances in the course of a metal titration [6,7,10,196,252].

In the region of slow exchange on the chemical shift time scale each exchanging species gives a separate signal that can be monitored individually. Only very few metal binding motifs have been characterized so far that are able to slow down exchange so significantly. Among them are the strong binding sites in the stem of G-quadruplex structures, for which lifetimes can be exceptionally long on the NMR chemical shift timescale [227,228] and which have been studied extensively due to their compact size.

In slowly exchanging systems, the frequency differences between bound and unbound species directly indicate lower limits for residence times, even if the fully bound state is usually not reached. In this way directly observed G-quadruplex channel-bound and free $^{23}Na^{+}$ and $^{85}Rb^{+}$ resonances gave conservative lower residence limits of 90 µs and 17 µs, respectively [237].

Similarly, the shifts of the K^+-substitute $^{205}Tl^+$ allows estimation of exchange rates in a G-quartet, where also one especially slowly exchanging ion could be identified through the exceptionally small line width [239]. Slow exchange is also amenable to saturation transfer experiments. Monitoring the efficiency of magnetization transfer from free $^{205}Tl^+$ to bound $^{205}Tl^+$ for varying saturation times, bound lifetimes between 80 ± 10 ms and 155 ± 65 ms for different binding sites on a G-quadruplex were found [193]. Employing $^{15}NH_4^+$, ^{15}N–^1H N_z exchange HSQC experiments at incremented mixing times allow the observation of different ammonia species – free and bound via inner- and outersphere binding in the channel permitting the quantification of the exchange rates between the individual species [229,253,254]. A considerably slower exchange for $^{15}NH_4^+$ than for Na^+ is observed.

The binding rates of the anticancer drug *cis*-diamminedichloroplatinum(II) and its *trans* isomer, however, are on a completely different time scale than any of the slowly-exchanging examples above. To illustrate this: binding kinetics in the range of 10^{-5} s^{-1} are determined from the gradually growing peaks of the mono- and bifunctional Pt^{2+}-DNA adducts over many hours [255].

5.2. Further Methods

NMR is the by far most used method to study metal ion binding kinetics in nucleic acids and there are only few examples where a different approach has led to the determination of association-dissociation rates. Dynamics in the µs-range are fast on the NMR, but not necessarily on the EPR time scale and thus exchange processes that are averaged out in the former, might be resolved in the latter [167].

Labuda and Pörschke have used the intrinsic fluorescence of the wyosine (Wye) nucleobase, which is a natural modification of guanine, to establish binding kinetics of Mg^{2+} and Ca^{2+} to the anticodon loop in tRNA [256]. By a temperature jump method, relaxation parameters in the absence and presence of metal ions were determined. Interestingly, the rate constants for Ca^{2+} binding in general and Mg^{2+} innersphere binding particularly were found to be in the ms range.

Where experimental methods reach their limits in terms of resolution and exchange rates,

molecular dynamics (MD) simulations can give complementary information on the metal binding to known nucleic acid structures. However, the force field description of di- and multivalent cations is much more demanding than that of monovalent ions [257]. In addition, at present, simulations are limited to below μs time scales, which is too short to observe, e.g., the dehydration of Mg^{2+} [258]. What is possible in terms of kinetics, however, is the evaluation of the residence times of the more easily dehydrated K^+ and Na^+ with nucleic acid surfaces that happen on the ps to ns time scale [259–262] and for longer-lived bound metal species the estimation of lower boundaries of residence times [263].

6. DETERMINATION OF BINDING AFFINITIES

Two challenges are faced in the thermodynamic analysis of metal ion binding to nucleic acids. Firstly, metal ion binding is inextricably interwoven with the folding and structural stability of nucleic acids and the one cannot be studied without affecting the other [264]. Secondly, usually there are only few specific binding sites with higher affinity and they coexist with a large background of weak, transient electrostatic interactions that are not easily accounted for in simple binding polynomials [265]. Both problems can sometimes be alleviated by determining apparent affinity constants under moderately high monovalent salt conditions, assuming that then the nucleic acid conformation will not significantly change any more upon addition of the metal ion to be analyzed and that all unspecific interaction sites will be saturated by the monovalent ion.

Metal ion affinities have been inferred from a range of different observables, like thermodynamic stabilities of the nucleic acid fold measured by UV melting curves [266–269] or the thermodynamics of folding of the hammerhead ribozyme by isothermal titration calorimetry (ITC) [270]. Qualitative and quantitative assessment of sequence specific ion binding to DNA A-tracts has been undertaken based on the reduced effective charge that can be detected by free solution capillary chromatography [271,272]. Apparent metal affinity constants have been determined from observed rate constants of ribozyme catalysis in many cases (e.g., [154,157,273–275]). An approach based on the gas-phase fragmentation of metal-nucleic acid

complexes in ESI-MS (electrospray ionization mass spectrometry) was recently applied to determine binding affinities to the thrombin binding aptamer [276]. In addition, the ratio of bound and unbound metal ions, as determined by fluorescent indicators, AES (atomic emission spectroscopy), NMR, EPR or lanthanide luminescence, in dependence of metal ion concentration, yields information on binding affinities (see Sections 6.1–6.3).

These various approaches differ in their ability to derive quantitative information, their ability to distinguish between multiple coexisting binding sites and their limits in terms of macromolecule size. All of the above methods yield signals that are an overlay of all the binding sites present in the system. Analysis of the dependence of the bound and free metal ion concentrations on the total metal ion concentration by, e.g., Hill or Scatchard plots can help to disentangle them to some extent to determine classes of binding sites with similar affinities and their occupancies and give information about binding cooperativity. However, one should be aware that reciprocal plots, like Scatchard or Eadie-Hofstee plots can lead to wrong values, as some experimental data points can obtain too much weight depending on their distribution [277]. In addition, this approach is in many cases challenged by the interdependence of RNA folding and metal ion binding [264]. Aside from that, there is usually also a restriction to simpler model molecules with one or only few strong binding sites. While the size restriction is also true for NMR, this method has one advantage over all the others: It allows to separately monitor binding events at several individual binding sites in a molecule and to determine intrinsic binding affinities (see Section 6.3).

6.1. Stoichiometric Methods – "Ion Counting"

So-called "ion counting" methods detect the free metal ion concentration in a sample, from which the number of ions strongly bound to the nucleic acid can be deduced. This can be useful to establish the number of strong divalent metal ion binding sites in a high-salt background [143], but also to evaluate the affinities of different metal ions with respect to each other. Here, fluorescent indicators have been widely used to determine free metal ion concentrations [278–280]. However, such dyes are usually restricted to the detection of one specific kind of metal ion. Recent methodological progress has made AES a very valuable tool in this regard, able to detect

a far wider range of mono- and divalent cations and also anions, thereby more completely accounting for the ion cloud around polynucleotides [281,282]. Irrespective of the way of detection, those methods are based on the equilibration of the nucleic acid-containing solution (by dialysis or ultrafiltration spin columns) against a buffer solution with well defined metal content. After the equilibrium is reached, metal ion concentrations in both solutions are measured and the number of metal ions retained per nucleic acid molecule can be determined [278,282].

6.2. Relative Affinities by Competition Experiments

EPR, lanthanide luminescence or NMR experiments can be used to directly sense the bound metal ions. All these methods, however, are restricted to certain metal ions each: EPR mainly to Mn^{2+}, which can differ significantly from Mg^{2+} in binding affinities for nucleic acid ligands [167], luminescence measurements to lanthanide(III) ions, mainly Tb^{3+}, and NMR to NMR-active nuclei. Competition experiments, where the observable ion is displaced stepwise by increasing concentration of another (silent) metal ion, can yield relative apparent affinities for a wider range of ions [275,283–285]. The same method can also be applied, for example, in Tb^{3+} cleavage experiments: The change in cleavage intensity with increasing amounts of competing Mg^{2+} can in principle be used to calculate Mg^{2+} binding affinity at specific sites [9,10].

6.3. Calculating Site-Specific Intrinsic Binding Affinities from NMR Chemical Shifts

While slow exchange can make things easier in the study of binding kinetics, for the determination of affinity constants by NMR fast exchange can be advantageous. Observable nuclei that are affected by the fast exchange between the metal-bound and metal-free state exhibit one resonance at the population-weighted average position. Titration with a metal ion will shift the free-to-bound equilibrium and thereby the position of the peak. Similarly, the peak width of a resonance will be affected when the titrated metal ion is paramagnetic. If a resonance is influenced only by one single association-dissociation event, the chemical shift change or change in peak width, respectively, plotted against metal ion concentration can be fitted by a 1:1

binding isotherm using e.g. a Levenberg-Marquardt [7,196,286,287] or a Newton-Gauss [288] algorithm and binding constants can be deduced. This has been widely used for small complexes [25,27,40,86,289–291], as well as for more complicated nucleic acids [7].

However, if there is more than one binding site all having similar affinities, as is usually always the case for nucleic acids, the sites will compete for the metal ions. Therefore the effective metal ion concentration that is available for each binding site at each titration step is lower than what was actually added and calculated affinities will always be underestimated. An iterative approach proposed by Erat, Sigel et al. circumvents this caveat (Figure 7) [7,9,10]. The first step is the grouping of resonances, according to their initial affinity constants and additional information like Mn^{2+} line broadening, into probable binding sites. The average binding constants for those sites are used to determine a refined free metal ion concentration. The newly determined metal concentration is again inserted into the calculation of binding constants. These steps are repeated until the calculated affinities do not significantly change any more.

insert Figure 7 close to here (width: 11.5 cm)

Proton resonances lend themselves to this kind of study because of their easy and fast acquisition, comparably good signal dispersion in 2D experiments and high sensitivity to changes in their environment. However, there are some factors that can hamper the determination of binding constants in this way. Firstly, bound Mg^{2+} exchanges with the solvent on the intermediate NMR chemical shift time scale and lines can get too broad to follow at higher concentrations. Secondly, the presumption that each binding site is affected by a single binding event is often not true, especially for protons. A second binding event close-by or a structural rearrangement, even if it is small, can make the data unusable. And thirdly, of course, the mapping of binding sites requires that resonances have been assigned.

7. EFFECTS OF OTHER FACTORS

7.1. Effect of Anions

The stabilities of commonly employed metal salts have to be kept in mind when characterizing

and quantifying cation-nucleic acid interactions. Adverse effects are possible especially in the high, non-physiological concentrations of certain salts that are part of many setups and can interfere with the collection of quantitative information. For example, the group of DeRose observes significant coordination of Mn^{2+} to Cl^- at high Cl^- concentrations [167]. Similarly, Cd^{2+} is known to form a rather stable $CdCl^+$ complex in aqueous solution: Consequently, an increase in Cd^{2+} affinity towards RNA of 0.8 log unit for log K_A values has been observed for M^{2+} binding to the bulge region within the catalytic domain 5 of a group II intron ribozyme when using 100 $KClO_4$ instead of 100 mM KCl [292].

Compared to cations, information on anion binding to nucleic acids is rather scarce, even though they too have been shown to be present in the first coordination shell of nucleic acids. Molecular dynamics simulations and a thorough evaluation of crystal structures [293–295] have identified anions (Cl^-, SO_4^{2-}, ClO_4^-, and PO_4^{3-} as the most frequently employed anions in crystallization buffers and MD simulations). These anions replace water molecules close to nucleobase amino groups as well as to endocyclic nitrogens and 2'-OH groups. The same authors [295] also speculated that anions occupy sites that are also possible binding sites for the negatively charged functional groups of proteins, drugs or phosphate backbone groups from a distant nucleic acid strand.

Anions are also found in close association with metal ions [293,295]. In some cases local arrangements where the anion is situated between two cations suggest an interdependence of binding, where the anion facilitates the close approach of two positive charges (Figure 8) [295]. Close contact of two Mg^{2+} ions is observed in many ribozyme active sites. In some cases, based on abnormally short metal-metal distances and molecular dynamics simulations, the existence of a bridging hydroxide has been suspected [296–298].

insert Figure 8 in color close to here (width: 11.5 cm)

Nucleic acids are commonly studied in solutions containing Cl^-, SO_4^{2-}, ClO_4^- or PO_4^{3-}, yet little is known about the differential effects those anions might have on their physical properties. A study of ^{25}Mg relaxation revealed a different behavior in the presence of Cl^- and SO_4^{2-}, which is attributed to a lyotropic effect [234]. A difference between these two anions was also observed in the first step of splicing in a group II intron [299]. While ammonium chloride stimulated

branching readily, ammonium sulfate did so only after a long lag phase in reactivity.

7.2. Effect of Buffers

Metal ion complexation by a buffer is often neglected, but in fact rather common and can severely hamper the quantitative analysis of binding events (e.g., [300,301]). Many buffers commonly employed in biological applications interact significantly with metal ions [302-309]. The preparation of RNA or DNA samples for further experiments usually involves high amounts of Tris (2-amino-2-hydroxymethyl-propane-1,3-diol) and Hepes [N-(2- hydroxyethyl)-piperazine-N′-2-ethanesulfonic acid] [310], e.g., in transcription and electrophoresis running buffers, that have to be removed carefully before any quantitative investigation of metal ion binding is attempted [307] (Figure 9). When applying Mg^{2+}, buffers like Tris or Bistris [bis-(2-hydroxy-ethyl)-amino-tris(hydroxymethyl)-methane] have relatively little influence, but this changes when Ca^{2+} [39,311], 3d metal ions or Cd^{2+} are applied [39,57,307,308], which show an increased affinity, e.g., by about 2 log units for Cd^{2+}, if compared with Mg^{2+} [307]. Phosphate, which is frequently employed as a buffer in spectroscopic or biochemical experiments of nucleic acids, also interacts with metal ions strongly enough to falsify measurements of intrinsic affinity constants [36] or of reaction rates [312–315], an observation that holds for other buffers as well [312,316]. Consequently, one is often forced to work in buffer-free media [312,317,318].

insert Figure 9 close to here (width: 11 cm)

Not only metal ions engage in interactions with buffer molecules, but also nucleic acids have been shown to form complexes with certain buffers, which can lead to complex formation or affect the conformation [319,320]. Thus also the formation of nucleic acid ternary complexes with buffers and metal ions, like they have been observed for nucleotides [57,307,308,311,321] and in human serum albumin [322], is a possibility that should be kept in mind when studying the interactions of metal ions and nucleic acids.

7.3. Effects of Solvent Permittivity and Co-solutes to Mimic Macromolecular Crowding

Two more factors are of importance when evaluating the significance of *in vitro* findings for

metal ion nucleic acid interactions of biological systems: The dilute aqueous reaction conditions under which most *in vitro* investigations of nucleic acids take place are quite unrealistic with regard to the molecular crowding present in the cytoplasm and inside cellular organelles [323,324]. Also dielectric constants at the surface and even more in the interior of proteins and nucleic acids differ significantly from the value of about 80 for water. Depending on the local environment values between 20 to 70 can occur [325–330].

Studies in an aqueous solution of 1,4-dioxane have been used to simulate the reduced permittivity of such conditions and found an overall increased Mg^{2+} affinity to a short RNA hairpin [331]. Such an increase was also observed for the binding of Cu^{2+} to single nucleotides in dioxane-enriched solutions [332]. To simulate the crowded cellular environment, Nakano et al. investigated the stability and catalytic activity of a minimal hammerhead ribozyme with PEG8000 as co-solute [333,334]. The authors find that large neutral co-solutes stabilize the tertiary structure and enhance catalytic rates especially at low Mg^{2+} concentrations. In general, molecular crowding is expected to reduce the high concentrations of Mg^{2+} that are usually required for the correct folding of RNA molecules under *in vitro* conditions, when considering the situation in a living cell [335].

8. CONCLUDING REMARKS

Compared to the situation in most metalloproteins, metal ion binding to nucleic acids is rather weak and of a highly dynamic nature. The reason for such true binding equilibria are the nature of the ligands – mainly phosphates, aromatic ring nitrogen atoms, and bridging water molecules – and of the metal ions, i.e. alkaline and alkaline earth metal ions. In addition, the metal ions of interest are mostly spectroscopically silent, which makes their detection at the coordinating sites very difficult. Taken together, the detailed characterization of metal ion binding to nucleic acids is rather challenging. In this review we summarized the methods applied nowadays with the aim to understand metal ion binding in solution and compiled the literature for the more interested reader. It is obvious that we are not only far from understanding this fascinating interaction and thus also the folded structure and mechanism of action of nucleic acids, but also that the methods applied carry numerous caveats. Most studies rely on the application of *other* metal ions than,

e.g., Mg^{2+}, which automatically means that the system under investigation has been altered. Every kind of metal ion has its distinct coordinating properties and thus also the functional RNA will slightly (or possibly more seriously) change its structure and other properties. In order to draw conclusions how the system works in its wild-type form, i.e., in the presence of Mg^{2+}, one has to know exactly how the coordinating properties of the different metal ions change according to their position in the periodic table. Some efforts in this direction have been made and some progress was achieved in the past few years [8,34,37]. However, to make things more complicated, it also turned out that there seems to be no general rule: While for two different hammerhead ribozymes a clear correlation was found between cleavage rate and phosphate affinities of specific metal ions [34], no such correlation could be established for the *glms* ribozyme, which is about the same size and uses the same mechanism of cleavage [54]. Consequently, it looks like as if every ribozyme, sometimes even of the same class but from different organisms, has its own specificities for metal ion binding.

Most methods applied today find their origin in applications in the metalloprotein field and certainly many more will be transferred, adjusted, and applied to nucleic acids. There is a great need for the development of new methods to investigate metal ion binding to nucleic acids. Recent novel approaches include the use of electrospray ionization mass spectrometry (ESI-MS) [276]: Metal ion-nucleic acid complexes of the thrombin-binding aptamer of different concentration were fragmented in the gas-phase and such the binding affinities determined. Another recent approach makes use of a specifically placed nitroxide spin label in order to measure the distance to coordinated paramagnetic metal ions by EPR [168]. This latter method has been used repeatedly with proteins (e.g., [336–340]). It will be fascinating to see what other methods will come up in the near and also more distant future to help to solve the "mysteries" of metal ion binding to nucleic acids.

ACKNOWLEDGMENT

Financial support by the European Research Council (ERC Starting Grant 2010 to RKOS), the Swiss National Science Foundation (RKOS), the Swiss State Secretariat for Education and

Research within the COST Action D39 (RKOS) and the University of Zürich is gratefully acknowledged.

ABBREVIATIONS AND DEFINITIONS

5'UTR	5' untranslated region
AES	atomic emission spectroscopy
Bistris	bis-(2-hydroxy-ethyl)-amino-tris(hydroxymethyl)-methane
ENDOR	electron-nuclear double resonance spectroscopy
EPR	electron paramagnetic resonance
ER	endoplasmic reticulum
ESEEM	electron spin echo envelope modulation
ESI-MS	electrospray ionization mass spectrometry
EXAFS	extended X-ray absorption fine structure
FT-IR	Fourier-transform infrared
glmS	glucosamine-6-phosphate activated ribozyme
GNA	glycol nucleic acid
GTP	guanosine 5'-triphosphate
HDV	hepatitits delta virus
Hepes	(N-(2-hydroxyethyl)-piperazine-N′-2-ethanesulfonic acid
HSQC	heteronuclear singel quantum coherence
IR	infrared
ITC	isothermal titration calorimetry
MD	molecular dynamics
MOPS	3-(N-morpholino)propanesulfonic acid
MRD	magnetic relaxation dispersion
NAIM	nucleotide analog interference mapping
NLPB	non-linear Poisson-Boltzmann
NMR	nuclear magnetic resonance

NOE	nuclear Overhauser effect
NOESY	nuclear Overhauser effect spectroscopy
NTPαS	nucleoside 5'-α-thiotriphosphate
PAGE	polyacrylamide gel electrophoresis
PNA	peptide nucleic acid
RNase	ribonuclease
ROESY	rotating frame Overhauser effect spectroscopy
rRNA	ribosomal RNA
RzB	trans cleaving derivative of the hammerhead ribozyme from the peach latent mosaic viroid (PLMVd)
SRP	signal recognition particle
T5PNP	5′-*p*-nitrophenylphosphate
TFA	thermodynamic fingerprint analysis
Tris	2-amino-2-hydroxymethyl-propane-1,3-diol
tRNA	transfer RNA
Wye	wyosine, a natural analog of guanine
XANES	X-ray absorption near edge structure
XAS	X-ray absorption spectroscopy

REFERENCES

1. D. E. Draper, D. Grilley, A. M. Soto, *Annu. Rev. Biophys. Biomol. Struct.* **2005**, *34*, 221–243.
2. G. S. Manning, *Acc. Chem. Res.* **1979**, *12*, 443–449.
3. K. Chin, K. A. Sharp, B. Honig, A. M. Pyle, *Nat. Struct. Biol.* **1999**, *6*, 1055–1061.
4. S. A. Woodson, *Curr. Opin. Chem. Biol.* **2005**, *9*, 104–109.
5. V. K. Misra, R. Shiman, D. E. Draper, *Biopolymers* **2003**, *69*, 118–136.
6. R. K. O. Sigel, D. G. Sashital, D. L. Abramovitz, A. G. Palmer III, S. E. Butcher, A. M. Pyle, *Nat. Struct. Mol. Biol.* **2004**, *11*, 187–192.

7. M. C. Erat, R. K. O. Sigel, *Inorg. Chem.* **2007**, *46*, 11224–11234.
8. R. K. O. Sigel, H. Sigel, *Acc. Chem. Res.* **2010**, *43*, 974–984.
9. M. C. Erat, J. Coles, C. Finazzo, B. Knobloch, R. K. O. Sigel, *submitted for publication* **2011**.
10. M. C. Erat, R. K. O. Sigel, *Met. Ions Life Sci.* **2011**, *9*, 37–100.
11. N. V. Hud, V. Sklenár, J. Feigon, *J. Mol. Biol.* **1999**, *286*, 651–660.
12. L. McFail-Isom, C. C. Sines, L. D. Williams, *Curr. Opin. Struct. Biol.* **1999**, *9*, 298–304.
13. T. Theophanides, H. A. Tajmir-Riahi, *J. Biomol. Struct. Dyn.* **1985**, *2*, 995–1004.
14. M. Guéron, J. P. Demaret, M. Filoche, *Biophys. J.* **2000**, *78*, 1070–1083.
15. B. Spingler, *Chimia* **2009**, *63*, 153–156.
16. B. Spingler, C. da Pieve, *Dalton Trans.* **2005**, 1637–1643.
17. B. A. Armitage, *Nature Chem. Biol.* **2007**, *3*, 203–204.
18. M. J. Cromie, Y. X. Shi, T. Latifi, E. A. Groisman, *Cell* **2006**, *125*, 71–84.
19. C. E. Dann III, C. A. Wakeman, C. L. Sieling, S. C. Baker, I. Irnov, W. C. Winkler, *Cell* **2007**, *130*, 878–892.
20. J.-H. Chen, R. Yajima, D. M. Chadalavada, E. Chase, P. C. Bevilacqua, B. L. Golden, *Biochemistry* **2010**, *49*, 6508–6518.
21. N. Toor, K. S. Keating, S. D. Taylor, A. M. Pyle, *Science* **2008**, *320*, 77–82.
22. N. J. Reiter, A. Osterman, A. Torres-Larios, K. K. Swinger, T. Pan, A. Mondragon, *Nature* **2010**, *468*, 784–789.
23. M. R. Stahley, S. A. Strobel, *Science* **2005**, *309*, 1587–1590.
24. R. K. O. Sigel, A. M. Pyle, *Chem. Rev.* **2007**, *107*, 97–113.
25. R. K. O. Sigel, E. Freisinger, B. Lippert, *J. Biol. Inorg. Chem.* **2000**, *5*, 287–299.
26. R. K. O. Sigel, M. Sabat, E. Freisinger, A. Mower, B. Lippert, *Inorg. Chem.* **1998**, *38*, 1481–1490.
27. B. Knobloch, R. K. O. Sigel, B. Lippert, H. Sigel, *Angew. Chem., Int. Ed.* **2004**, *43*, 3793–3795.
28. B. Lippert, *Prog. Inorg. Chem.* **2005**, *54*, 385–443.
29. B. Lippert, *Chem. Biodivers.* **2008**, *5*, 1455–1474.

30. R. Griesser, G. Kampf, L. E. Kapinos, S. Komeda, B. Lippert, J. Reedijk, H. Sigel, *Inorg. Chem.* **2003**, *42*, 32–41.

31. H. Sigel, *Pure Appl. Chem.* **2004**, *76*, 1869–1886.

32. R. G. Pearson, *J. Chem. Edu.* **1968**, *45*, 643–648.

33. R. G. Pearson, *J. Chem. Edu.* **1968**, *45*, 581–587.

34. J. Schnabl, R. K. O. Sigel, *Curr. Opin. Chem. Biol.* **2010**, *14*, 269–275.

35. R. B. Martin, *Met. Ions Biol. Syst.* **1996**, *32*, 61–89.

36. R. K. O. Sigel, H. Sigel, *Met. Ions Life Sci.* **2007**, *2*, 109–180.

37. E. Freisinger, R. K. O. Sigel, *Coord. Chem. Rev.* **2007**, *251*, 1834–1851.

38. C. P. Da Costa, H. Sigel, *Inorg. Chem.* **2000**, *39*, 5985–5993.

39. F. M. Al-Sogair, B. P. Operschall, A. Sigel, H. Sigel, J. Schnabl, R. K. O. Sigel, *Chem. Rev.* **2011**, *111*, available online, doi: 10.1021/cr100415s.

40. A. Mucha, B. Knobloch, M. Jeżowska-Bojczuk, H. Kozłowski, R. K. O. Sigel, *Dalton Trans.* **2008**, 5368–5377.

41. L. A. Finney, T. V. O'Halloran, *Science* **2003**, *300*, 931–936.

42. S. J. Lippard, J. M. Berg, *Principles of Bioinorganic Chemistry*, University Science Books, Mill Valley, Ca, 1995.

43. *The Biological Chemistry of Magnesium*, Ed J. A. Cowan, VCH Publishers, Inc., New York, 1995.

44. T. Pan, D. M. Long, O. C. Uhlenbeck, in *The RNA World*, Eds R. Gesteland, J. Atkins, Cold Spring Harbor Press, Cold Spring Harbor, 1993, pp. 271–302.

45. R. L. Gonzalez, Jr., I. Tinoco, Jr., *Methods Enzymol.* **2001**, *338*, 421–443.

46. I. Tinoco, Jr., C. Bustamante, *J. Mol. Biol.* **1999**, *293*, 271–281.

47. A. M. Pyle, *Nature* **1996**, *381*, 280–281.

48. A. M. Pyle, *J. Biol. Inorg. Chem.* **2002**, *7*, 679–690.

49. R. K. O. Sigel, *Eur. J. Inorg. Chem.* **2005**, *12*, 2281–2292.

50. C. Hsiao, in *Nucleic Acid-Metal Ion Interactions*, Ed N. V. Hud, Royal Society of Chemistry, Cambridge, UK, 2009, pp. 1–38.

51. A. S. Petrov, J. C. Bowman, S. C. Harvey, L. D. Williams, *RNA* **2011**, *17*, 291–297.

52. M. Roychowdhury-Saha, D. H. Burke, *RNA* **2006**, *12*, 1846–1852.

53. J. L. Boots, M. D. Canny, E. Azimi, A. Pardi, *RNA* **2008**, *14*, 2212–2222.

54. K. Klawuhn, J. A. Jansen, J. Souchek, G. A. Soukup, J. K. Soukup, *ChemBioChem* **2010**, *11*, 2567–2571.

55. V. K. Misra, D. E. Draper, *Proc. Natl. Acad. Sci. USA* **2001**, *98*, 12456–12461.

56. K. Juneau, E. Podell, D. J. Harrington, T. R. Cech, *Structure* **2001**, *9*, 221–231.

57. H. Sigel, R. Griesser, *Chem. Soc. Rev.* **2005**, *34*, 875–900.

58. S. Basu, R. P. Rambo, J. Strauss-Soukup, J. H. Cate, A. R. Ferré-D'Amaré, S. A. Strobel, J. A. Doudna, *Nat. Struct. Biol.* **1998**, *5*, 986–992.

59. J. R. Williamson, M. K. Raghuraman, T. R. Cech, *Cell* **1989**, *59*, 871–880.

60. T. Pozzan, R. Rizzuto, *Nat. Cell Biol.* **2000**, *2*, E25–E27.

61. C. E. Outten, T. V. O'Halloran, *Science* **2001**, *292*, 2488–2492.

62. T. D. Rae, P. J. Schmidt, R. A. Pufahl, V. C. Culotta, T. V. O'Halloran, *Science* **1999**, *284*, 805–808.

63. B. Lippert, in *Nucleic Acid-Metal Ion Interactions*, Ed N. V. Hud, Royal Society of Chemistry, Cambridge, UK, 2009, pp. 39–74.

64. M. C. Erat, R. K. O. Sigel, *J. Biol. Inorg. Chem.* **2008**, *13*, 1025–1036.

65. H. Irving, R. J. P. Williams, *J. Chem. Soc.* **1953**, 3192–3210.

66. R. B. Martin, *Met. Ions Biol. Syst.* **1986**, *20*, 21–65.

67. R. B. Martin, *J. Chem. Edu.* **1987**, *64*, 402–402.

68. R. D. Shannon, *Acta Crystallogr.* **1976**, *A32*, 751–767.

69. *The Chemistry of Aqua Ions*, Ed D. T. Richens, John Wiley & Sons, Hoboken, 1997, pp. 592.

70. S. F. Lincoln, A. E. Merbach, *Adv. Inorg. Chem.* **1995**, *42*, 1–88.

71. C. F. Baes, Jr., R. E. Mesmer, *The Hydrolysis of Cations*, Krieger Publishing Co., Malabar, Florida, 1976, pp. 1–496.

72. R. G. Pearson, *Inorg. Chem.* **1988**, *27*, 734–740.

73. W. E. Morf, W. Simon, *Helv. Chim. Acta* **1971**, *54*, 794–810.

74. K. B. Yatsimirsky, *Theor. Exp. Chem.* **1994**, *30*, 1–11.

75. L. Helm, A. E. Merbach, *Chem. Rev.* **2005**, *105*, 1923–1959.
76. J. E. Huheey, *Inorganic Chemistry*, Harper and Row, New York, 1983.
77. Y. Inada, A. M. Mohammed, H. H. Loeffler, S. Funahashi, *Helv. Chim. Acta* **2005**, *88*, 461–469.
78. A. F. Holleman, E. Wiberg, *Lehrbuch der Anorganischen Chemie*, Walter de Gruyter, Berlin, New York, 1985, pp. 1265–1279.
79. Y. Peeraer, A. Rabijns, J.-F. Collet, E. Van Schaftingen, C. De Ranter, *Eur. J. Biochem.* **2004**, *271*, 3421–3427.
80. R. M. Weinshilboum, F. A. Raymond, *Biochem. Pharmacol.* **1976**, *25*, 573–579.
81. S.-o. Shan, D. Herschlag, *RNA* **2000**, *6*, 795–813.
82. M. Steiner, D. Rueda, R. K. O. Sigel, *Angew. Chem., Int. Ed.* **2009**, *48*, 9739–9742.
83. K. Aoki, *Acta Crystallogr. B* **1976**, *32*, 1454–1459.
84. V. L. Pecoraro, J. D. Hermes, W. W. Cleland, *Biochemistry* **1984**, *23*, 5262–5271.
85. R. K. O. Sigel, B. Song, H. Sigel, *J. Am. Chem. Soc.* **1997**, *119*, 744–755.
86. B. Knobloch, B. Nawrot, A. Okruszek, R. K. O. Sigel, *Chem. Eur. J.* **2008**, *14*, 3100–3109 and *14*, 3509.
87. H. Sigel, R. B. Martin, *Chem. Soc. Rev.* **1994**, *23*, 83–91.
88. A. T. Perrotta, M. D. Been, *Biochemistry* **2007**, *46*, 5124–5130.
89. N. Lehman, G. F. Joyce, *Nature* **1993**, *361*, 182–185.
90. N. Lehman, G. F. Joyce, *Curr. Biol.* **1993**, *3*, 723–734.
91. D. N. Frank, N. R. Pace, *Proc. Natl. Acad. Sci. USA* **1997**, *94*, 14355–14360.
92. B. Cuenoud, J. W. Szostak, *Nature* **1995**, *375*, 611–614.
93. N. Carmi, L. A. Shultz, R. R. Breaker, *Chem. Biol.* **1996**, *3*, 1039–1046.
94. W. Wang, L. P. Billen, Y. Li, *Chem. Biol.* **2002**, *9*, 507–517.
95. P. J. Bruesehoff, J. Li, A. J. Augustine, Y. Lu, *Comb. Chem. High T. Scr.* **2002**, *5*, 327–335.
96. J. Li, W. C. Zheng, A. H. Kwon, Y. Lu, *Nucleic Acids Res.* **2000**, *28*, 481–488.
97. T. Pan, B. Dichtl, O. C. Uhlenbeck, *Biochemistry* **1994**, *33*, 9561–9565.
98. H. P. Hofmann, S. Limmer, V. Hornung, M. Sprinzl, *RNA* **1997**, *3*, 1289–1300.

99. M. Zivarts, Y. Liu, R. R. Breaker, *Nucleic Acids Res.* **2005**, *33*, 622–631.

100. Y. Lu, J. W. Liu, J. Li, P. J. Bruesehoff, C. M. B. Pavot, A. K. Brown, *Biosens. Bioelectron.* **2003**, *18*, 529–540.

101. T. Li, E. Wang, S. Dong, *Anal. Chem.* **2010**, *82*, 1515–1520.

102. B. Rosenberg, L. Vancamp, J. E. Trosko, V. H. Mansour, *Nature* **1969**, *222*, 385–386.

103. A. M. Pizarro, P. J. Sadler, in *Nucleic Acid-Metal Ion Interactions*, Ed N. V. Hud, Royal Society of Chemistry, Cambridge, UK, 2009, pp. 350–416.

104. A. Ono, S. Cao, H. Togashi, M. Tashiro, T. Fujimoto, T. Machinami, S. Oda, Y. Miyake, I. Okamoto, Y. Tanaka, *Chem. Commun.* **2008**, 4825–4827.

105. A. Ono, H. Togashi, *Angew. Chem. Int. Ed.* **2004**, *43*, 4300–4302.

106. J. Liu, Y. Lu, *Angew. Chem. Int. Ed.* **2007**, *46*, 7587–7590.

107. X. Liu, Y. Tang, L. Wang, J. Zhang, S. Song, C. Fan, S. Wang, *Adv. Mat.* **2007**, *19*, 1471–1474.

108. R. Freeman, T. Finder, I. Willner, *Angew. Chem. Int. Ed.* **2009**, *48*, 7818–7821.

109. T. Carell, C. Behrens, J. Gierlich, *Org. Biomol. Chem.* **2003**, *1*, 2221–2228.

110. J. S. Lee, L. J. Latimer, R. S. Reid, *Biochem. Cell Biol.* **1993**, *71*, 162–168.

111. P. Aich, S. L. Labiuk, L. W. Tari, L. J. T. Delbaere, W. J. Roesler, K. J. Falk, R. P. Steer, J. S. Lee, *J. Mol. Biol.* **1999**, *294*, 477–485.

112. A. Rakitin, P. Aich, C. Papadopoulos, Y. Kobzar, A. S. Vedeneev, J. S. Lee, J. M. Xu, *Phys. Rev. Lett.* **2001**, *86*, 3670–3673.

113. F. Moreno-Herrero, P. Herrero, F. Moreno, J. Colchero, C. Gómez-Navarro, J. Gómez-Herrero, A. M. Baró, *Nanotechnology* **2003**, *14*, 128–128.

114. M. Fuentes-Cabrera, B. G. Sumpter, J. E. Šponer, J. Šponer, L. Petit, J. C. Wells, *J. Phys. Chem. B* **2007**, *111*, 870–879.

115. S. S. Alexandre, J. M. Soler, L. Seijo, F. Zamora, *Phys. Rev. B* **2006**, *73*, 205112–205112.

116. S. L. Labiuk, L. T. J. Delbaere, J. S. Lee, *J. Biol. Inorg. Chem.* **2003**, *8*, 715–720.

117. Y. Tanaka, S. Oda, H. Yamaguchi, Y. Kondo, C. Kojima, A. Ono, *J. Am. Chem. Soc.* **2007**, *129*, 244–245.

118. S. Johannsen, N. Megger, D. Böhme, R. K. O. Sigel, J. Müller, *Nature Chem.* **2010**, *2*,

229–234.

119. Y. Miyake, H. Togashi, M. Tashiro, H. Yamaguchi, S. Oda, M. Kudo, Y. Tanaka, Y. Kondo, R. Sawa, T. Fujimoto, T. Machinami, A. Ono, *J. Am. Chem. Soc.* **2006**, *128*, 2172–2173.
120. E. Ennifar, P. Walter, P. Dumas, *Nucleic Acids Res.* **2003**, *31*, 2671–2682.
121. D. Böhme, N. Düpre, D. A. Megger, J. Müller, *Inorg. Chem.* **2007**, *46*, 10114–10119.
122. K. Tanaka, A. Tengeiji, T. Kato, N. Toyama, M. Shiro, M. Shionoya, *J. Am. Chem. Soc.* **2002**, *124*, 12494–12498.
123. G. H. Clever, C. Kaul, T. Carell, *Angew. Chem. Int. Ed.* **2007**, *46*, 6226–6236.
124. G. H. Clever, K. Polborn, T. Carell, *Angew. Chem. Int. Ed.* **2005**, *44*, 7204–7208.
125. J. Müller, *Eur. J. Inorg. Chem.* **2008**, 3749–3763.
126. G. H. Clever, M. Shionoya, *Coord. Chem. Rev.* **2010**, *254*, 2391–2402.
127. F. H. Westheimer, *Acc. Chem. Res.* **1968**, *1*, 70–78.
128. G. A. Soukup, R. R. Breaker, *RNA* **1999**, *5*, 1308–1325.
129. R. S. Brown, J. C. Dewan, A. Klug, *Biochemistry* **1985**, *24*, 4785–4801.
130. R. Breslow, D.-L. Huang, *Proc. Natl. Acad. Sci. USA* **1991**, *88*, 4080–4083.
131. C. Werner, B. Krebs, G. Keith, G. Dirheimer, *Biochim. Biophys. Acta* **1976**, *432*, 161–175.
132. R. S. Brown, B. A. Hingerty, J. C. Dewan, A. Klug, *Nature* **1983**, *303*, 543–546.
133. J. Ciesiolka, W. D. Hardt, J. Schlegl, V. A. Erdmann, R. K. Hartmann, *Eur. J. Biochem.* **1994**, *219*, 49–56.
134. M. Hertweck, M. W. Müller, *Eur. J. Biochem.* **2001**, *268*, 4610–4620.
135. J. Ciesiolka, T. Marciniec, W. J. Krzyzosiak, *Eur. J. Biochem.* **1989**, *182*, 445–450.
136. R. K. O. Sigel, A. Vaidya, A. M. Pyle, *Nat. Struct. Biol.* **2000**, *7*, 1111–1116.
137. R. K. O. Sigel, A. M. Pyle, *Met. Ions Biol. Syst.* **2003**, *40*, 477–512.
138. I. Zagórowska, S. Kuusela, H. Lönnberg, *Nucleic Acids Res.* **1998**, *26*, 3392–3396.
139. C. Berens, B. Streicher, R. Schroeder, W. Hillen, *Chem. Biol.* **1998**, *5*, 163–175.
140. H. J. H. Fenton, *Proc. Chem. Soc.* **1893**, *9*, 113–113.
141. H. J. H. Fenton, *J. Chem. Soc.* **1894**, *65*, 899–910.
142. I. D. Brown, *Acta Crystallogr. B* **1988**, *44*, 545–553.

143. R. Das, K. J. Travers, Y. Bai, D. Herschlag, *J. Am. Chem. Soc.* **2005**, *127*, 8272–8273.

144. I. T. Suydam, S. A. Strobel, *Methods Enzymol.* **2009**, *468*, 3–30.

145. E. L. Christian, M. Yarus, *Biochemistry* **1993**, *32*, 4475–4480.

146. S. Basu, S. A. Strobel, *Methods* **2001**, *23*, 264–275.

147. J. A. Jansen, T. J. McCarthy, G. A. Soukup, J. K. Soukup, *Nature Struct. Mol. Biol.* **2006**, *13*, 517–523.

148. V. D. Sood, T. L. Beattie, R. A. Collins, *J. Mol. Biol.* **1998**, *282*, 741–750.

149. A. D. Griffiths, B. V. Potter, I. C. Eperon, *Nucleic Acids Res.* **1987**, *15*, 4145–4162.

150. C. P. Da Costa, D. Krajewska, A. Okruszek, W. J. Stec, H. Sigel, *J. Biol. Inorg. Chem.* **2002**, *7*, 405–415.

151. C. P. Da Costa, A. Okruszek, H. Sigel, *ChemBioChem* **2003**, *4*, 593–602.

152. J. K. Frederiksen, R. Fong, J. A. Piccirilli, in *Nucleic Acid-Metal Ion Interactions*, Ed N. V. Hud, Royal Society of Chemistry, Cambridge, UK, 2009, pp. 260–306.

153. S. Basu, S. A. Strobel, *RNA* **1999**, *5*, 1399–1407.

154. S.-O. Shan, A. Yoshida, S. Sun, J. A. Piccirilli, D. Herschlag, *Proc. Natl. Acad. Sci. USA* **1999**, *96*, 12299–12304.

155. J. K. Frederiksen, J. A. Piccirilli, *Methods* **2009**, *49*, 148–166.

156. M. Forconi, D. Herschlag, *Methods Enzymol.* **2009**, *468*, 311–333.

157. S. Wang, K. Karbstein, A. Peracchi, L. Beigelman, D. Herschlag, *Biochemistry* **1999**, *38*, 14363–14378.

158. W. W. Cleland, in *Enzyme Kinetics and Mechanism Part D: Developments in Enzyme Dynamics*, Ed D. L. Purich, Academic Press, 1995, Vol. 249, pp. 341–373.

159. D. B. Northrop, *Methods* **2001**, *24*, 117–124.

160. A. G. Cassano, V. E. Anderson, M. E. Harris, *Biochemistry* **2004**, *43*, 10547–10559.

161. A. G. Cassano, V. E. Anderson, M. E. Harris, *Biopolymers* **2004**, *73*, 110–129.

162. M. E. Harris, A. G. Cassano, *Curr. Opin. Chem. Biol.* **2008**, *12*, 626–639.

163. Q. Dai, J. K. Frederiksen, V. E. Anderson, M. E. Harris, J. A. Piccirilli, *J. Org. Chem.* **2008**, *73*, 309–311.

164. J. L. Leroy, M. Guéron, *Biopolymers* **1977**, *16*, 2429–2446.

165. T. E. Horton, D. R. Clardy, V. J. DeRose, *Biochemistry* **1998**, *37*, 18094–18101.

166. N. Kisseleva, S. Kraut, A. Jaschke, O. Schiemann, *HFSP J.* **2007**, *1*, 127–136.

167. L. Hunsicker-Wang, M. Vogt, V. J. DeRose, *Methods Enzymol.* **2009**, *468*, 335–367.

168. V. J. DeRose, in *Nucleic Acid-Metal Ion Interactions*, Ed N. V. Hud, Royal Society of Chemistry, Cambridge, UK, 2009, pp. 154–179.

169. M. Vogt, S. Lahiri, C. G. Hoogstraten, R. D. Britt, V. J. DeRose, *J. Am. Chem. Soc.* **2006**, *128*, 16764–16770.

170. J. E. Penner-Hahn, *Coord. Chem. Rev.* **2005**, *249*, 161–177.

171. I. V. Smirnov, F. W. Kotch, I. J. Pickering, J. T. Davis, R. H. Shafer, *Biochemistry* **2002**, *41*, 12133–12139.

172. K. S. Koutmou, A. Casiano-Negroni, M. M. Getz, S. Pazicni, A. J. Andrews, J. E. Penner-Hahn, H. M. Al-Hashimi, C. A. Fierke, *Proc. Natl. Acad. Sci. USA* **2010**, *107*, 2479–2484, S2479/2471–S2479/2475.

173. B.-K. Teo, P. Eisenberger, J. Reed, J. K. Barton, S. J. Lippard, *J. Am. Chem. Soc.* **1978**, *100*, 3225–3227.

174. A. P. Hitchcock, C. J. L. Lock, W. M. C. Pratt, *Inorg. Chim. Acta* **1982**, *66*, L45–L47.

175. J. M. Benevides, S. A. Overman, G. J. Thomas, *J. Raman Spec.* **2005**, *36*, 279–299.

176. T. Theophanides, in *Infrared and Raman Spectroscopy of Biological Materials*, Ed H.-U. Gremlich, B. Yan, M. Dekker, New York, 2000, pp. 205–223.

177. Y. Chen, N. V. Eldho, K. T. Dayie, P. R. Carey, *Biochemistry* **2010**, *49*, 3427–3435.

178. H. Takeuchi, H. Murata, I. Harada, *J. Am. Chem. Soc.* **1988**, *110*, 392–397.

179. H. A. Tajmir-Riahi, T. Theophanides, *J. Biomol. Struct. Dyn.* **1985**, *3*, 537–542.

180. S. Adam, P. Bourtayre, J. Liquier, E. Taillandier, *Nucleic Acids Res.* **1986**, *14*, 3501–3513.

181. M. Langlais, H. A. Tajmir-Riahi, R. Savoie, *Biopolymers* **1990**, *30*, 743–752.

182. J. Duguid, V. A. Bloomfield, J. Benevides, G. J. Thomas, *Biophys. J.* **1993**, *65*, 1916–1928.

183. J. G. Duguid, V. A. Bloomfield, J. M. Benevides, G. J. Thomas, *Biophys. J.* **1995**, *69*, 2623–2641.

184. H. Arakawa, J. F. Neault, H. A. Tajmir-Riahi, *Biophys. J.* **2001**, *81*, 1580–1587.

185. J. Stangret, R. Savoie, *Phys. Chem. Chem. Phys.* **2002**, *4*, 4770–4773.

186. S. Nafisi, Z. Norouzi, *DNA Cell Biol.* **2009**, *28*, 469–477.

187. S. Nafisi, A. Sobhanmanesh, K. Alimoghaddam, A. Ghavamzadeh, H.-A. Tajmir-Riahi, *DNA Cell Biol.* **2005**, *24*, 634–640.

188. E. L. Christian, V. E. Anderson, P. R. Carey, M. E. Harris, *Biochemistry* **2010**, *49*, 2869–2879.

189. J.-H. Chen, B. Gong, P. C. Bevilacqua, P. R. Carey, B. L. Golden, *Biochemistry* **2009**, *48*, 1498–1507.

190. B. Gong, J.-H. Chen, E. Chase, D. M. Chadalavada, R. Yajima, B. L. Golden, P. C. Bevilacqua, P. R. Carey, *J. Am. Chem. Soc.* **2007**, *129*, 13335–13342.

191. B. Gong, Y. Chen, E. L. Christian, J. H. Chen, E. Chase, D. M. Chadalavada, R. Yajima, B. L. Golden, P. C. Bevilacqua, P. R. Carey, *J. Am. Chem. Soc.* **2008**, *130*, 9670–9672.

192. A. Wong, R. Ida, G. Wu, *Biochem. Biophys. Res. Commun.* **2005**, *337*, 363–366.

193. M. L. Gill, S. A. Strobel, J. P. Loria, *J. Am. Chem. Soc.* **2005**, *127*, 16723–16732.

194. R. L. J. Gonzalez, I. Tinoco, Jr., *Methods Enzymol.* **2002**, *338*, 421–443.

195. J. Feigon, S. E. Butcher, L. D. Finger, N. V. Hud, *Methods Enzymol.* **2001**, *338*, 400–420.

196. M. C. Erat, O. Zerbe, T. Fox, R. K. O. Sigel, *ChemBioChem* **2007**, *8*, 306–314.

197. S. E. Butcher, F. H.-T. Allain, J. Feigon, *Biochemistry* **2000**, *39*, 2174–2182.

198. P. Legault, C. G. Hoogstraten, E. Metlitzky, A. Pardi, *J. Mol. Biol.* **1998**, *284*, 325–335.

199. M. Seetharaman, N. V. Eldho, R. A. Padgett, K. T. Dayie, *RNA* **2006**, *12*, 235–247.

200. M. Schmitz, I. Tinoco Jr., *RNA* **2000**, *6*, 1212–1225.

201. R. L. Gonzalez, Jr., I. Tinoco Jr., *J. Mol. Biol.* **1999**, *289*, 1267–1282.

202. S. S. Wijmenga, B. N. M. van Buuren, *Prog. Nucl. Mag. Res. Sp.* **1998**, *32*, 287–387.

203. B. A. Connolly, F. Eckstein, *Biochemistry* **1984**, *23*, 5523–5527.

204. M. K. Hansen, J.-P. Simorre, P. Hanson, V. Mokler, L. Bellon, L. Beigelman, A. Pardi, *RNA* **1999**, *5*, 1099–1104.

205. F. Eckstein, *Annu. Rev. Biochem.* **1985**, *54*, 367–402.

206. M. C. Erat, R. K. O. Sigel, *results to be published*.

207. M. Maderia, L. M. Hunsicker, V. J. DeRose, *Biochemistry* **2000**, *39*, 12113–12120.

208. E. M. Osborne, W. L. Ward, M. Z. Ruehle, V. J. DeRose, *Biochemistry* **2009**, *48*, 10654–10664.

209. Y. Tanaka, C. Kojima, E. H. Morita, Y. Kasai, K. Yamasaki, A. Ono, M. Kainosho, K. Taira, *J. Am. Chem. Soc.* **2002**, *124*, 4595–4601.

210. G. Wang, B. L. Gaffney, R. A. Jones, *J. Am. Chem. Soc.* **2004**, *126*, 8908–8909.

211. G. W. Buchanan, J. B. Stothers, *Can. J. Chem.* **1982**, *60*, 787–791.

212. Y. Tanaka, Y. Kasai, S. Mochizuki, A. Wakisaka, E. H. Morita, C. Kojima, A. Toyozawa, Y. Kondo, M. Taki, Y. Takagi, A. Inoue, K. Yamasaki, K. Taira, *J. Am. Chem. Soc.* **2004**, *126*, 744–752.

213. Y. Tanaka, E. H. Morita, H. Hayashi, Y. Kasai, T. Tanaka, K. Taira, *J. Am. Chem. Soc.* **2000**, *122*, 11303–11310.

214. M. C. Erat, H. Kovacs, R. K. O. Sigel, *J. Inorg. Biochem.* **2010**, *104*, 611–613.

215. V. Sychrovský, J. Šponer, P. Hobza, *J. Am. Chem. Soc.* **2004**, *126*, 663–672.

216. H. Li, R. I. Cukier, Y. Bu, *J. Phys. Chem. B* **2008**, *112*, 9174–9181.

217. I. Bertini, C. Luchinat, *NMR of Paramagnetic Molecules in Biological Systems*, Benjamin/Cummings Pub. Co., Menlo Park, CA, 1986, pp. 319.

218. I. Bertini, C. Luchinat, G. Parigi, *Solution NMR of Paramagnetic Molecules - Applications to Metallobiomolecules and Models*, Elsevier Science B.V., Amsterdam, 2001, pp. 1–372.

219. J. H. Davis, T. R. Foster, M. Tonelli, S. E. Butcher, *RNA* **2007**, *13*, 76–86.

220. J. Noeske, H. Schwalbe, J. Wöhnert, *Nucleic Acids Res.* **2007**, *35*, 5262–5273.

221. D. O. Campbell, P. Bouchard, G. Desjardins, P. Legault, *Biochemistry* **2006**, *45*, 10591–10605.

222. R. E. Hurd, E. Azhderian, B. R. Reid, *Biochemistry* **1979**, *18*, 4012–4017.

223. J. A. Cowan, *J. Inorg. Biochem.* **1993**, *49*, 171–175.

224. G. Colmenarejo, I. Tinoco Jr., *J. Mol. Biol.* **1999**, *290*, 119–135.

225. J. S. Kieft, I. Tinoco, Jr., *Structure* **1997**, *5*, 713–721.

226. S. Rüdisser, I. Tinoco, Jr., *J. Mol. Biol.* **2000**, *295*, 1211–1223.

227. P. Schultze, N. V. Hud, F. W. Smith, J. Feigon, *Nucleic Acids Res.* **1999**, *27*, 3018–3028.

228. F. W. Smith, J. Feigon, *Biochemistry* **1993**, *32*, 8682–8692.

229. N. V. Hud, P. Schultze, V. Sklenár, J. Feigon, *J. Mol. Biol.* **1999**, *285*, 233–243.

230. D. M. Rose, C. F. Polnaszek, R. G. Bryant, *Biopolymers* **1982**, *21*, 653–664.

231. S. S. Reid, J. A. Cowan, *Biochemistry* **1990**, *29*, 6025–6032.

232. E. Berggren, L. Nordenskiöld, W. H. Braunlin, *Biopolymers* **1992**, *32*, 1339–1350.

233. J. A. Cowan, H. W. Huang, L. Y. Hsu, *J. Inorg. Biochem.* **1993**, *52*, 121–129.

234. L. A. Wright, L. E. Lerner, *Biopolymers* **1994**, *34*, 691–700.

235. L. M. Utschig, J. W. Bryson, T. V. O'Halloran, *Science* **1995**, *268*, 380–385.

236. J. E. Coleman, *Methods Enzymol.* **1993**, *227*, 16–43.

237. R. Ida, G. Wu, *J. Am. Chem. Soc.* **2008**, *130*, 3590–3602.

238. J. P. André, H. R. Mäcke, *J. Inorg. Biochem.* **2003**, *97*, 315–323.

239. S. Basu, A. A. Szewczak, M. Cocco, S. A. Strobel, *J. Am. Chem. Soc.* **2000**, *122*, 3240–3241.

240. J. Reedijk, *Platinum Metals Review* **2008**, *52*, 2–11.

241. L. Helm, A. E. Merbach, *Coord. Chem. Rev.* **1999**, *187*, 151–181.

242. L.-Y. Lian, G. C. K. Roberts, in *NMR of Macromolecules: A Practical Approach*, Ed G. C. K. Roberts, IRL Press at Oxford University Press, Oxford, New York, 1993, pp. 153–182.

243. H. S. Gutowsky, C. H. Holm, *J. Chem. Phys.* **1956**, *25*, 1228–1228.

244. L. Nordenskiold, D. K. Chang, C. F. Anderson, M. T. Record, *Biochemistry* **1984**, *23*, 4309–4317.

245. W. H. Braunlin, C. F. Anderson, M. T. Record, *Biochemistry* **1987**, *26*, 7724–7731.

246. W. H. Braunlin, T. Drakenberg, L. Nordenskiöld, *Biopolymers* **1987**, *26*, 1047–1062.

247. B. Halle, V. P. Denisov, *Biopolymers* **1998**, *48*, 210–233.

248. B. Halle, V. P. Denisov, *Methods Enzymol.* **2002**, *338*, 178–201.

249. V. P. Denisov, G. Carlström, K. Venu, B. Halle, *J. Mol. Biol.* **1997**, *268*, 118–136.

250. V. P. Denisov, B. Halle, *Proc. Natl. Acad. Sci. USA* **2000**, *97*, 629–633.

251. F. Cesare Marincola, V. P. Denisov, B. Halle, *J. Am. Chem. Soc.* **2004**, *126*, 6739–6750.

252. S. Johannsen, M. M. T. Korth, J. Schnabl, R. K. O. Sigel, *Chimia* **2009**, *63*, 146–152.

253. P. Podbevšek, N. V. Hud, J. Plavec, *Nucleic Acids Res.* **2007**, *35*, 2554–2563.

254. P. Šket, J. Plavec, *J. Am. Chem. Soc.* **2007**, *129*, 8794–8800.

255. D. P. Bancroft, C. A. Lepre, S. J. Lippard, *J. Am. Chem. Soc.* **1990**, *112*, 6860–6871.

256. D. Labuda, D. Poerschke, *Biochemistry* **1982**, *21*, 49–53.

257. S. E. McDowell, N. Špačková, J. Šponer, N. G. Walter, *Biopolymers* **2007**, *85*, 169–184.

258. Y. Hashem, P. Auffinger, *Methods* **2009**, *47*, 187–197.

259. P. Auffinger, L. Bielecki, E. Westhof, *J. Mol. Biol.* **2004**, *335*, 555–571.

260. P. Auffinger, E. Westhof, *J. Mol. Biol.* **2000**, *300*, 1113–1131.

261. P. Auffinger, N. Grover, E. Westhof, *Met. Ions Life Sci.* **2011**, *9*, 1–35.

262. P. Várnai, K. Zakrzewska, *Nucleic Acids Res.* **2004**, *32*, 4269–4280.

263. M. V. Krasovska, J. Sefcikova, K. Reblova, B. Schneider, N. G. Walter, J. Šponer, *Biophys. J.* **2006**, *91*, 626–638.

264. V. K. Misra, D. E. Draper, *J. Mol. Biol.* **2002**, *317*, 507–521.

265. D. E. Draper, *RNA* **2004**, *10*, 335–343.

266. M. J. Serra, J. D. Baird, T. Dale, B. L. Fey, K. Retatagos, E. Westhof, *RNA* **2002**, *8*, 307–323.

267. Y. V. Bukhman, D. E. Draper, *J. Mol. Biol.* **1997**, *273*, 1020–1031.

268. R. Shiman, D. E. Draper, *J. Mol. Biol.* **2000**, *302*, 79–91.

269. L. G. Laing, T. C. Gluick, D. E. Draper, *J. Mol. Biol.* **1994**, *237*, 577–587.

270. C. Hammann, A. Cooper, D. M. J. Lilley, *Biochemistry* **2001**, *40*, 1423–1429.

271. Q. Dong, E. Stellwagen, N. C. Stellwagen, *Biochemistry* **2009**, *48*, 1047–1055.

272. N. C. Stellwagen, S. Magnusdottir, C. Gelfi, P. G. Righetti, *J. Mol. Biol.* **2001**, *305*, 1025–1033.

273. P. M. Gordon, E. J. Sontheimer, J. A. Piccirilli, *Biochemistry* **2000**, *39*, 12939–12952.

274. S.-I. Nakano, D. J. Proctor, P. C. Bevilacqua, *Biochemistry* **2001**, *40*, 12022–12038.

275. A. K. Brown, J. Li, C. M. B. Pavot, Y. Lu, *Biochemistry* **2003**, *42*, 7152–7161.

276. J. M. Wilcox, D. L. Rempel, M. L. Gross, *Anal. Chem.* **2008**, *80*, 2365–2371.

277. R. B. Martin, *J. Chem. Ed.* **1997**, *74*, 1238–1240.

278. D. Grilley, A. M. Soto, D. E. Draper, *Methods Enzymol.* **2009**, *455*, 71–94.

279. H. Krakauer, *Biopolymers* **1971**, *10*, 2459–2490.

280. R. Römer, R. Hach, *Eur. J. Biochem.* **1975**, *55*, 271–284.

281. Y. Bai, M. Greenfeld, K. J. Travers, V. B. Chu, J. Lipfert, S. Doniach, D. Herschlag, *J. Am. Chem. Soc.* **2007**, *129*, 14981–14988.

282. M. Greenfeld, D. Herschlag, *Methods Enzymol.* **2009**, *469*, 375–389.

283. L. M. Hunsicker, V. J. DeRose, *J. Inorg. Biochem.* **2000**, *80*, 271–281.

284. M. L. Bleam, C. F. Anderson, M. T. Record, Jr., *Proc. Natl. Acad. Sci. USA* **1980**, *77*, 3085–3089.

285. A. L. Feig, M. Panek, W. D. Horrocks, Jr., O. C. Uhlenbeck, *Chem. Biol.* **1999**, *6*, 801–810.

286. K. Levenberg, *Quart. Appl. Math.* **1944**, *2*, 164–168.

287. D. W. Marquardt, *SIAM J. Appl. Math.* **1963**, *11*, 431–431.

288. R. Tribolet, H. Sigel, *Eur. J. Biochem.* **1987**, *163*, 353–363.

289. B. Knobloch, W. Linert, H. Sigel, *Proc. Natl. Acad. Sci. USA* **2005**, *102*, 7459–7464.

290. B. Knobloch, H. Sigel, A. Okruszek, R. K. O. Sigel, *Chem. Eur. J.* **2007**, *13*, 1804–1814.

291. B. Knobloch, D. Suliga, A. Okruszek, R. K. O. Sigel, *Chem. Eur. J.* **2005**, *11*, 4163–4170.

292. B. Knobloch, M. C. Erat, R. K. O. Sigel, *to be submitted for publication*.

293. P. Auffinger, L. Bielecki, E. Westhof, *Structure* **2004**, *12*, 379–388.

294. M. Feig, B. M. Pettitt, *Biophys. J.* **1999**, *77*, 1769–1781.

295. J. S. Kieft, E. Chase, D. A. Costantino, B. L. Golden, *RNA* **2010**, *16*, 1118–1123.

296. T. Hermann, P. Auffinger, W. G. Scott, E. Westhof, *Nucleic Acids Res.* **1997**, *25*, 3421–3427.

297. M. Boero, J. M. Park, Y. Hagiwara, M. Tateno, *J. Phys. Cond. Matter* **2007**, *19*, 365217–365217.

298. C. C. Correll, B. Freeborn, P. B. Moore, J. A. Steitz, *Cell* **1997**, *91*, 705–712.

299. K. Chin, A. M. Pyle, *RNA* **1995**, *1*, 391–406.

300. C. Montigny, P. Champeil, *Anal. Biochem.* **2007**, *366*, 96–98.

301. P. Leverrier, C. Montigny, M. Garrigos, P. Champeil, *Anal. Biochem.* **2007**, *371*, 215–228.

302. D. P. Hanlon, D. S. Watt, E. W. Westhead, *Anal. Biochem.* **1966**, *16*, 225–233.

303. D. E. Allen, D. J. Baker, R. D. Gillard, *Nature* **1967**, *214*, 906–907.

304. R. Nakon, C. R. Krishnamoorthy, *Science* **1983**, *221*, 749–750.

305. P. D. Prenzler, W. D. McFadyen, *J. Inorg. Biochem.* **1997**, *68*, 279–282.

306. Q. Yu, A. Kandegedara, Y. Xu, D. B. Rorabacher, *Anal. Biochem.* **1997**, *253*, 50–56.

307. K. H. Scheller, T. H. J. Abel, P. E. Polanyi, P. K. Wenk, B. E. Fischer, H. Sigel, *Eur. J. Biochem.* **1980**, *107*, 455–466.

308. B. E. Fischer, U. K. Häring, R. Tribolet, H. Sigel, *Eur. J. Biochem.* **1979**, *94*, 523–530.

309. H. Sigel, K. H. Scheller, B. Prijs, *Inorg. Chim. Acta (Bioinorganic Chemistry)* **1982**, *66*, 147–155.

310. S. Gallo, M. Furler, R. K. O. Sigel, *CHIMIA* **2005**, *59*, 812–816.

311. P. Champeil, T. Menguy, S. Soulie, B. Juul, A. G. de Gracia, F. Rusconi, P. Falson, L. Denoroy, F. Henao, M. le Maire, J. V. Møller, *J. Biol. Chem.* **1998**, *273*, 6619–6631.

312. H. Sigel, *Coord. Chem. Rev.* **1990**, *100*, 453–539.

313. H. Sigel, F. Hofstetter, R. B. Martin, R. M. Milburn, V. Scheller-Krattiger, K. H. Scheller, *J. Am. Chem. Soc.* **1984**, *106*, 7935–7946.

314. H. Sigel, H. Erlenmeyer, *Helv. Chim. Acta* **1966**, *49*, 1266–1274.

315. H. Sigel, P. E. Amsler, *J. Am. Chem. Soc.* **1976**, *98*, 7390–7400.

316. P. E. Amsler, H. Sigel, *Eur. J. Biochem.* **1976**, *63*, 569–581.

317. H. Sigel, *Angew. Chem. Int. Ed.* **1969**, *8*, 167–177.

318. H. Sigel, C. Flierl, R. Griesser, *J. Am. Chem. Soc.* **1969**, *91*, 1061–1064.

319. K. L. Buchmueller, K. M. Weeks, *Nucleic Acids Res.* **2004**, *32*, e184–e184.

320. N. C. Stellwagen, A. Bossi, C. Gelfi, P. G. Righetti, *Anal. Biochem.* **2000**, *287*, 167–175.

321. N. A. Corfù, B. Song, L.-n. Ji, *Inorg. Chim. Acta* **1992**, *192*, 243–251.

322. M. Sokolowska, W. Bal, *J. Inorg. Biochem.* **2005**, *99*, 1653–1660.

323. K. Luby-Phelps, *Int. Rev. Cytol.* **2000**, *192*, 189–221.

324. N. A. Chebotareva, B. I. Kurganov, N. B. Livanova, *Biochemistry (Moscow)* **2004**, *69*, 1239–1251.

325. D. C. Rees, *J. Mol. Biol.* **1980**, *141*, 323–326.

326. N. K. Rogers, G. R. Moore, M. J. E. Sternberg, *J. Mol. Biol.* **1985**, *182*, 613–616.

327. H. Sigel, R. B. Martin, R. Tribolet, U. K. Haring, R. Malini-Balakrishnan, *Eur. J. Biochem.* **1985**, *152*, 187–193.

328. R. Jin, K. J. Breslauer, *Proc. Natl. Acad. Sci. USA* **1988**, *85*, 8939–8942.

329. M. A. Young, B. Jayaram, D. L. Beveridge, *J. Phys. Chem. B* **1998**, *102*, 7666–7669.

330. A. Okamoto, K. Tainaka, I. Saito, *Bioconjugate Chem.* **2005**, *16*, 1105–1111.

331. M. Furler, B. Knobloch, R. K. O. Sigel, *Inorg. Chim. Acta* **2009**, *362*, 771–776.

332. R. Tribolet, R. Malini-Balakrishnan, H. Sigel, *J. Chem. Soc., Dalton Trans., Inorg. Chem.* **1985**, 2291–2303.

333. S.-I. Nakano, H. T. Karimata, Y. Kitagawa, N. Sugimoto, *J. Am. Chem. Soc.* **2009**, *131*, 16881–16888.

334. S.-I. Nakano, Y. Kitagawa, H. T. Karimata, N. Sugimoto, *Nucleic Acids Symp. Ser.* **2008**, *52*, 519–520.

335. D. Kilburn, J. H. Roh, L. Guo, R. M. Briber, S. A. Woodson, *J. Am. Chem. Soc.* **2010**, *132*, 8690–8696.

336. D. J. Hirsh, G. W. Brudvig, *Nature Protocols* **2007**, *2*, 1770–1781.

337. H.-J. Steinhoff, *Biol. Chem.* **2011**, *385*, 913–920.

338. J. Voss, L. Salwiński, H. R. Kaback, W. L. Hubbell, *Proc. Natl. Acad. Sci. USA* **1995**, *92*, 12295–12299.

339. J. Voss, W. L. Hubbell, H. R. Kaback, *Proc. Natl. Acad. Sci. USA* **1995**, *92*, 12300–12303.

340. J. S. Leigh, *J. Chem. Phys.* **1970**, *52*, 2608–2608.

341. N. Toor, K. Rajashankar, K. S. Keating, A. M. Pyle, *Nature Struct. Mol. Biol.* **2008**, *15*, 1221–1222.

342. G. L. Conn, A. G. Gittis, E. E. Lattman, V. K. Misra, D. E. Draper, *J. Mol. Biol.* **2002**, *318*, 963–973.

343. G. W. Collie, S. M. Haider, S. Neidle, G. N. Parkinson, *Nucleic Acids Res.* **2010**, *38*, 5569–5580.

344. A. Gelasco, S. J. Lippard, *Biochemistry* **1998**, *37*, 9230–9239.

Table 1. Concentration of various metal ions in the ocean, mammalian cells, the extracellular space, as well as bacterial cells. The respective literature source is always given in the title row.

M^{n+}	Seawater [42] [ppm]	Seawater [43] [mM]	Mammalian cell [43] [mM]	Extracellular space [43] [mM]	Bacterial cells [44] [mg/kg]	Bacterial cytosol [41] [mM]
Li^+	0.17					
Na^+	$1.1 \cdot 10^4$	470	10	145	$4.6 \cdot 10^3$	
K^+	$3.9 \cdot 10^2$	10	140	5	$115 \cdot 10^3$	> 10
Rb^+	90					
Cs^+	3					
Be^{2+}	$6 \cdot 10^{-7}$					
Mg^{2+}	$1.35 \cdot 10^3$	50	30[a]	1	$7 \cdot 10^3$	> 10
Ca^{2+}	$4.1 \cdot 10^2$	10	1	4	$5.1 \cdot 10^3$	0.1
Sr^{2+}	375					
Ba^{2+}	425					
Cr^{2+}	$5 \cdot 10^{-4}$				4	
Mn^{2+}	$2 \cdot 10^{-3}$				260	10^{-2}
Fe^{2+}	$3 \cdot 10^{-3}$	$1 \cdot 10^{-4}$			170	0.1
Co^{2+}	$4 \cdot 10^{-4}$	$3.1 \cdot 10^{-6}$			7.5	low
Ni^{2+}	$7 \cdot 10^{-3}$	$1 \cdot 10^{-6}$				low
Cu^+						10^{-2}
Cu^{2+}	$3 \cdot 10^{-3}$	$1 \cdot 10^{-3}$			150	
Zn^{2+}	$1 \cdot 10^{-2}$	$1 \cdot 10^{-4}$			83	0.1
Ru^{3+}	$1 \cdot 10^{-2}$					
Pd^{2+}	$1 \cdot 10^{-2}$					
Ag^+	$7 \cdot 10^{-2}$					
Cd^{2+}	0.2				31	
Pt^{2+}	$1 \cdot 10^{-2}$					
Au^{3+}	$4 \cdot 10^{-3}$					
Hg^{2+}	$8 \cdot 10^{-2}$					
Tl^+	0.5					
Pb^{2+}	13					

[a] The free concentration of Mg^{2+} is about 1 mM.

Table 2. Collection of some physicochemical properties of metal ions, i.e., ionic radius, preferred coordination number (CN), water exchange rate from the first hydration shell (k_{ex} at 298 K), p$K_{a,aq}$ values of the bound water molecules, Pearson hardness (η), free enthalpy of hydration (ΔG_{hydr}), and for coordination number 6 also $\Delta G_{hydrCN6}$. The respective literature sources for the values are given in the top row.

M^{n+}	Ionic radius[a] [Å] [68]	Coordination numbers[b] [43,69]	Preferred ligands [10,43]	k_{ex} [s^{-1}] [70]	p$K_{a,aq}$ [71]	Pearson hardness [72]	ΔG_{hydr} [a] [kJ/mol] [73]	$\Delta G_{hydrCN6}$ [kJ/mol] [74]
Li^+	0.59	4		~10^9	13.64	35.1	–438	–509
Na^+	1.02 (1.18)	6 (8)		~10^9	14.18	21.1	–412 (–383)	–404
K^+	1.38 (1.51)	6 (8)		~10^9	14.46	13.6	–322 (–308)	–330
Rb^+	1.52, 1.61	6, 8		~10^9		11.6	–292, –279	–309
Cs^+	(1.67) 1.74	(6) 8		~10^9		10.6	(–269) –256	–287
Be^{2+}	0.27 (0.45)	4 (6)		730 (CN=4)	5.4	67.8	–2381 (–2218)	–2445
Mg^{2+}	0.72	6	O	5.3-6.6 · 10^5	11.44	32.6	–1858	–1883
Ca^{2+}	(1.06) 1.12	(6) 8	O	~10^9	12.85	19.5	(–1569) –1657	–1558
Sr^{2+}	(1.18) 1.26	(6) 8	O	~10^9	13.29	16.3	(–1385) –1460	–1452
Ba^{2+}	(1.35) 1.42	(6) 8	O	~10^9	13.47		(–1289) –1360	–1289
Cr^{2+}	0.80	6		~10^9		7.2		–1901
Cr^{3+}	0.62	6	O/N	2.4 · 10^{-6}	4	9.1	–4523	–4492
Mn^{2+}	0.67	6	O/N	2.1 · 10^7	10.59	9.0	–1761	–1821
Fe^{2+}	0.61, 0.78	ls 6, hs 6		4.39 · 10^6	9.5	7.2	–1870	–1911
Fe^{3+}	0.55, 0.65	ls 6, hs 6		1.6 · 10^2 / 10^{-3} [c]	0.7 (ls) / 2.19 (hs) [e]	12.1	–4469	–4352
Co^{2+}	0.58, 0.75	4, 6	O/N/S	3.18 · 10^6 (CN=6)	9.65	8.2	–1707, –1887	–1964
Co^{3+}	0.55, 0.61	ls 6, hs 6	O/N	~10^{-1} [e]		8.9		–4572
Ni^{2+}	0.55, 0.66 [c]	th 4, sq 4	O/N/S	3.15 · 10^4 (CN=6)	9.86	8.5	–1757 (–1950)	–2045
Cu^{1+}	0.77	6				6.3		–562
Cu^{2+}	0.73	6		4.4 · 10^9	>8	8.3		–2059
Zn^{2+}	0.60, 0.74	4, 6	O/N/S	4.1 · 108 [f]	8.96	10.9	–1690, –1870	–2007
Ru^{3+}	0.68	6		3.5 · 10^{-6}		10.7		
Pd^{2+}	0.64	sq 4		560	2.3 [c]	6.8		–1967
Ag^+	0.67, 1.02	2, sq 4			12.0	7.0	–335, –381	–468
Cd^{2+}	0.78, 0.95	4, 6	O/N/S	6.1 · 108 [f]	10.08	10.3	–1489, –1640	–1780
Pt^{2+}	0.60	4		7.1 · 10^{-6}	~2.5 [c]	8.0		–2059
Au^{3+}	0.68	4				8.4		–4353
Hg^{2+}	1.02	6		1.8 · 109 [f]	3.4	7.7	–1598	–1809
Tl^+	1.50	6			13.21	7.2	–329	–337
Pb^{2+}	1.19 (1.29)	6 (8)	O		7.71	8.5	–1431 (–1523)	–1477
Eu^{3+}	1.07, 1.12	8, 9 [d]	O		7.8		–3547 [g]	
Tb^{3+}	1.04	8 [d]	O	5.6 · 10^{-6} (CN=8)	7.9		–3605 [g]	

[a] The value in parentheses refers to the respective coordination number also given in parentheses in column 3. [b] If appropriate, low spin (ls) and high spin (hs) is distinguished. In the case of CN = 4, the square planer (sq) or tetrahedral (th) geometry is indicated. [c] Values taken from [69]. [d] Values taken from [75]. [e] Values taken from ref [76]. [f] Values taken from ref [77]. [g] Values taken from [78].

FIGURE LEGENDS

Figure 1. The five most common nucleobases in RNA and DNA: Guanine (gua/G), cytosine (cyt/C), adenine (ade/A), thymine (thy/T) and uracil (ura/U) are drawn as present in canonical Watson-Crick or wobble base pairs (top). The phosphate sugar backbone of DNA and RNA is depicted below. The most common metal ion coordination sites are indicated by bold letters.

Figure 2. Views of different metal ion binding sites in nucleic acids. (a) Two Mg^{2+} ions in the active site of a group II intron (light orange) coordinate the scissile bond of the substrate oligonucleotide (light green) (PDB ID 3G78; [341]). (b) Buried K^+ ion in its binding pocket as found in the crystal structure of a 58 nt long rRNA fragment (PDB ID 1HC8; [342]). (c) Top and side view of a G-quadruplex structure with two K^+ ions in its central channel (PDB ID 3IBK; [343]). (d) $[Co(NH_3)_6]^{3+}$ bound to the major groove of two G·U pairs, the amine ligands are shown in light green (PDB ID 1AJF; [225]). (e) Intrastrand *cis*-Pt(II) adduct with the Pt^{2+} coordinated to two guanine-N7 sites and two NH_3 ligands shown in light green (PDB ID 1A84; [344]). (f) Three consecutive Ag^+-mediated imidazole base pairs (PDB ID 2KE8; [118]). All panels were prepared using pymol (www.pymol.org) and the indicated PDB IDs.

Figure 3. Mechanism of RNA cleavage by a classical in-line attack. The nucleophillic 2'-OH attacks the adjacent phosphodiester and the opposite 5'-OH is liberated upon formation of 2',3'-cyclic phosphate in this S_{N2} reaction. The attacking nucleophile and the leaving group are positioned ideally in a 180° angle to achieve a maximum cleavage rate.

Figure 4. The use of NAIM analysis combined with thiorescue to identify metal ion binding sites in RNA. The example shown visualizes a phosphorothioate interference at position 2 and a nucleobase mutation at position 6 that both can be rescued by a thiophilic metal. The introduced thiophosphate group at position 5 cannot be rescued by the addition of a more thiophilic metal ion, indicating that this group undergoes another kind of crucial (but unknown) interaction within the three-dimensional architecture of the RNA. This Figure is adapted from [144].

Figure 5. Signatures of metal ion binding to nucleic acids as observed in NMR spectra. (a) Mg^{2+} interaction is indicated by chemical shift changes (titration from 0 mM, red, to 12 mM Mg^{2+}, dark

blue). Line broadening indicates direct Mg^{2+} coordination. The panel is adapted from [7] and [252]. (b) Selective line broadening is observed in a ^{1}H NMR spectrum with increasing amounts of Mn^{2+} (titration from 0 μM, blue, to 210 μM, yellow). (c) Coordination of a Ag^{+} ion causes a 86 Hz splitting of the imidazole N3 signal in a [^{1}H,^{15}N]-HSQC. Panel adapted from [118]. (d) Binding of $[Co(NH_3)_6]3^{+}$ can be observed by NOE crosspeaks between the protons of its ammine ligands (bulk resonance at 3.65 ppm) and the imino protons of a short RNA hairpin.

Figure 6. Depending on the exchange rate between two states and the respective resonances in their NMR spectrum, the two peaks fall together (top) or are clearly separated (bottom) as the two extremes.

Figure 7. Calculation of intrinsic affinity constants as deduced from chemical shift changes upon Mg^{2+} addition to a large RNA [7,9,10]. (a) Scheme of the iterative calculation procedure. (b) Fit of the experimental data from H6 of U21 in a group II intron domain 6 after the first and the fifth iteration [7]. The data points shift to the left, as the available Mg^{2+} concentration for each site becomes smaller. Simultaneously the calculated intrinsic affinity constant increases from log K_{A1} = 2.11 ± 0.09 to log K_{A5} = 2.52 ± 0.04 [7].

Figure 8. Anions bound to metal ion within nucleic acid structures. (a) A chloride ion (pink) bridges two $[Co(NH_3)_6]^{3+}$ complexes in the crystal structure of the *E.coli* signal recognition particle (SRP) RNA (PDB ID 3LQX; [295]). (b) A binuclear Mg^{2+} complex in the loop E motif is bridged by three water or hydroxide molecules, respectively (PDB ID 354D; [298]). The panels were prepared using pymol (www.pymol.org) and the indicated PDB IDs.

Figure 9. Buffers commonly employed in experiments of nucleic acids. All buffers are shown in their protonated form.

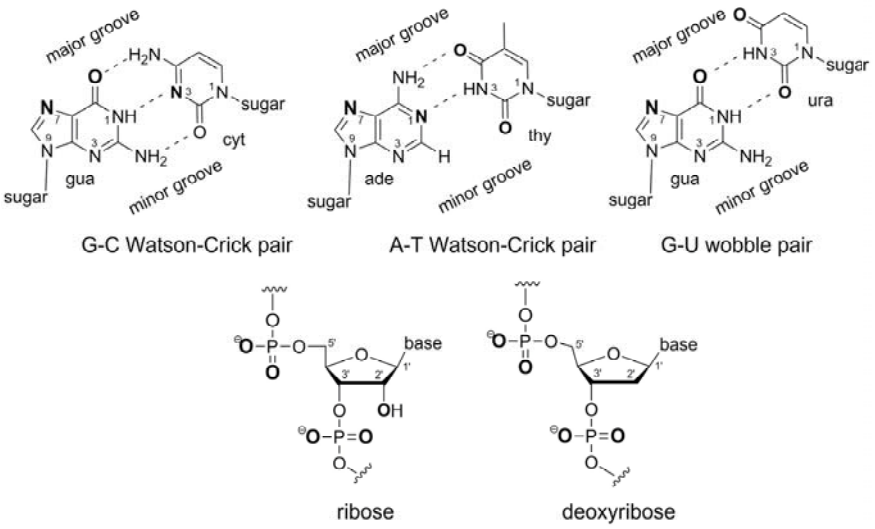
major groove
sugar
cyt
gua
minor groove
G-C Watson-Crick pair
ade
thy
A-T Watson-Crick pair
ura
G-U wobble pair
base
ribose
deoxyribose

Figure 1

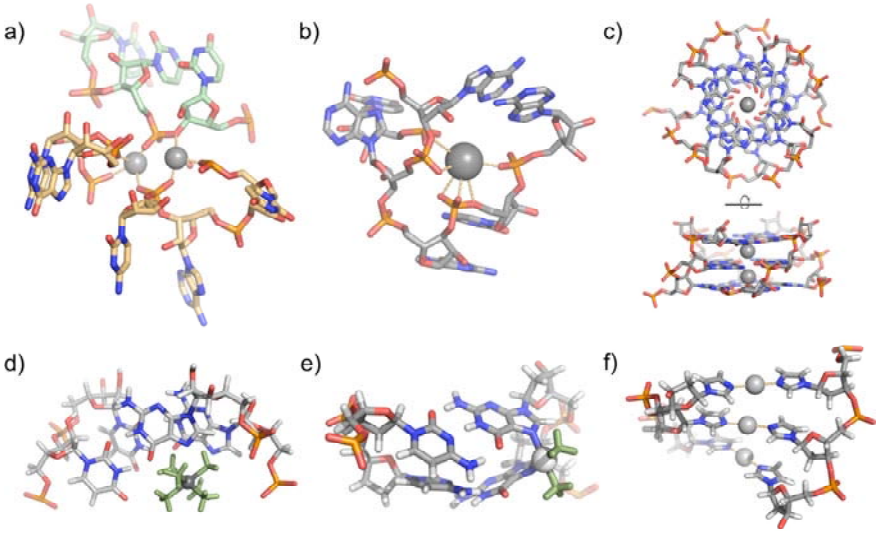

Figure 2

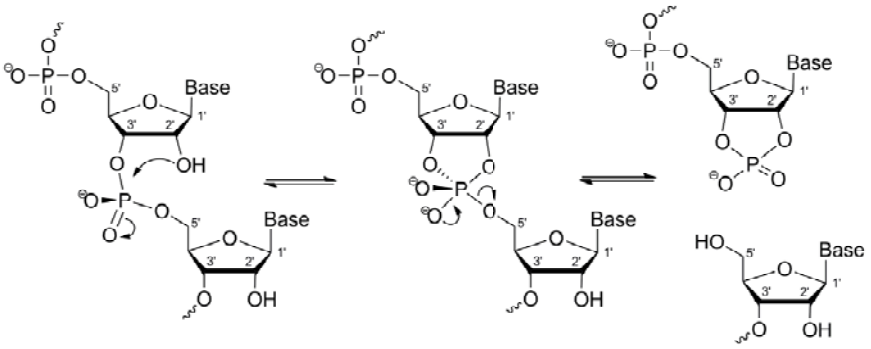

Figure 3

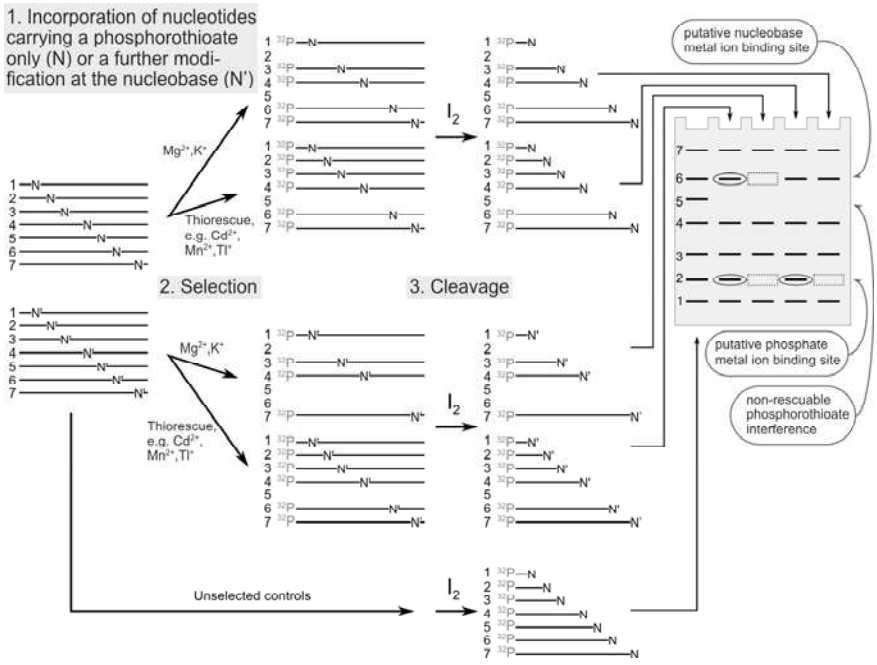
1. Incorporation of nucleotides carrying a phosphorothioate only (N) or a further modification at the nucleobase (N')
Mg2+,K+
Thiorescue, e.g. Cd2+, Mn2+,Tl+
I2
putative nucleobase metal ion binding site
2. Selection
3. Cleavage
putative phosphate metal ion binding site
non-rescuable phosphorothioate interference
Unselected controls

Figure 4

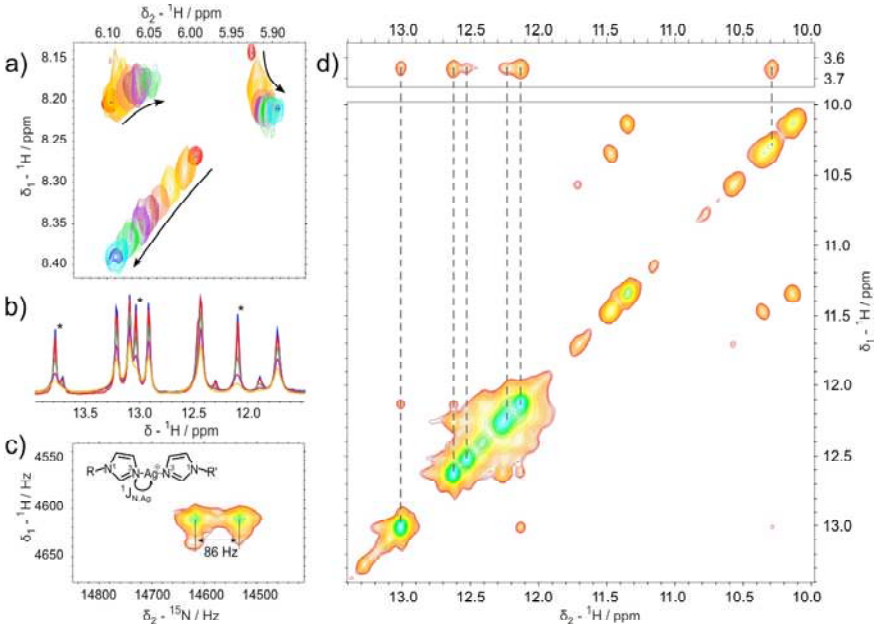
a)
b)
c)
d)
δ2 - 1H / ppm
δ1 - 1H / ppm
δ - 1H / ppm
δ1 - 1H / Hz
δ2 - 15N / Hz
δ2 - 1H / ppm
δ1 - 1H / ppm
1JN,Ag
86 Hz

Figure 5

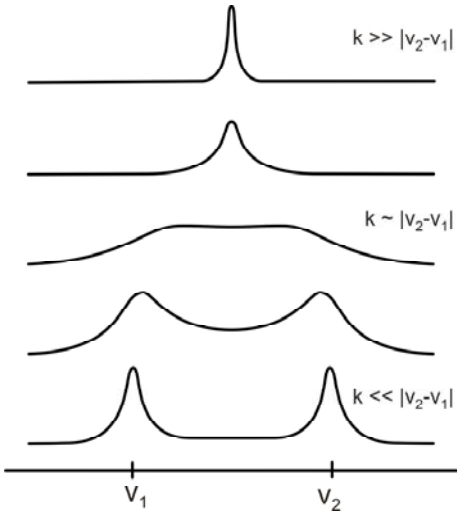

Figure 6

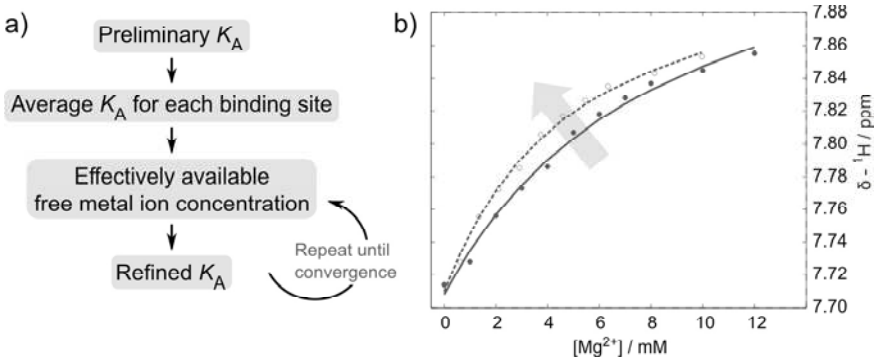
a)
Preliminary K_A
Average K_A for each binding site
Effectively available free metal ion concentration
Refined K_A
Repeat until convergence
b)
7.88
7.86
7.84
7.82
7.80
7.78
7.76
7.74
7.72
7.70
δ - ^{1}H / ppm
0
2
4
6
8
10
12
[Mg^{2+}] / mM

Figure 7

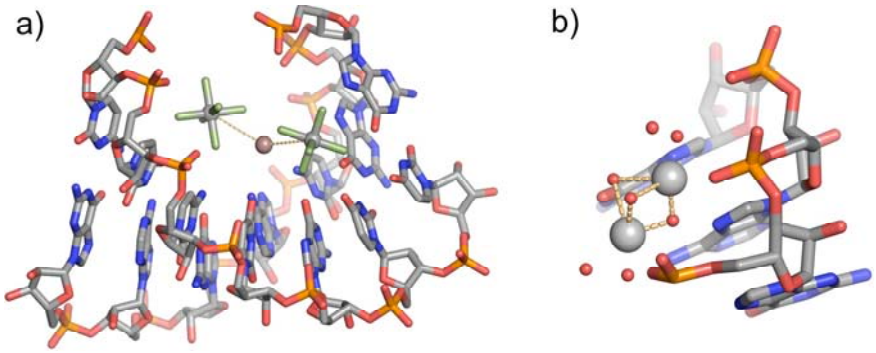

Figure 8

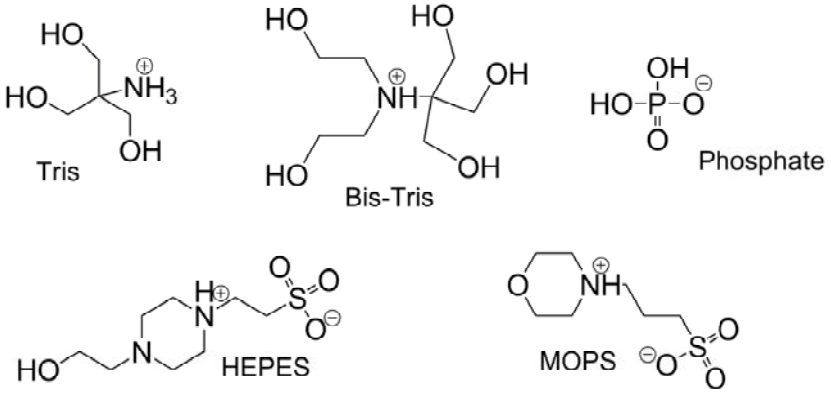
HO
HO
NH3
OH
Tris
HO
HO
NH
OH
HO
OH
Bis-Tris
OH
HO
P
O
O
Phosphate
H
N
O
S
O
O
N
HO
HEPES
O
NH
O
S
O
O
O
MOPS

Figure 9